

# Small fish biomass limits the catch potential in the High Seas

Jerome Guet<sup>1</sup>, Daniele Bianchi<sup>2</sup>, Kim Scherrer<sup>3</sup>, Ryan Heneghan<sup>4</sup>, and Eric D. Galbraith<sup>5</sup>

<sup>1</sup>University of California, Los Angeles

<sup>2</sup>University of California Los Angeles

<sup>3</sup>Autonomous University of Barcelona

<sup>4</sup>School of Science and Environment

<sup>5</sup>McGill University

March 05, 2024

## Abstract

The High Seas, lying beyond the boundaries of nations' Exclusive Economic Zones, cover the majority of the ocean surface and host roughly two thirds of marine primary production. Yet, only a small fraction of global wild fish catch comes from the High Seas, despite intensifying industrial fishing efforts. The surprisingly small fish catch could reflect economic features of the High Seas - such as the difficulty and cost of fishing in remote parts of the ocean surface - or ecological features resulting in a small biomass of fish relative to primary production. We use the coupled biological-economic model BOATS to estimate contributing factors, comparing observed catches with simulations where: (i) fishing cost depends on distance from shore and seafloor depth; (ii) catchability depends on seafloor depth or vertical habitat extent; (iii) regions with micronutrient limitation have reduced biomass production; (iv) the trophic transfer of energy from primary production to demersal food webs depends on depth; and (v) High Seas biomass migrates to coastal regions. Our results suggest that the most important features are ecological: demersal fish communities receive a large proportion of primary production in shallow waters, but very little in deep waters due to respiration by small organisms throughout the water column. Other factors play a secondary role, with migrations having a potentially large but uncertain role, and economic factors having the smallest effects. Our results stress the importance of properly representing the High Seas biomass in future fisheries projections, and clarify their limited role in global food provision.

# Small fish biomass limits the catch potential in the High Seas

J. Guet<sup>1</sup>, D. Bianchi<sup>1</sup>, K.J.N. Scherrer<sup>2</sup>, R.F. Heneghan<sup>3,4</sup> and E.D.  
Galbraith<sup>5</sup>

<sup>1</sup>Department of Atmospheric and Oceanic Sciences, University of California Los Angeles, CA, United States

<sup>2</sup>Department of Biological Sciences, University of Bergen, 5020 Bergen, Norway

<sup>3</sup>Australian Rivers Institute, School of Environment and Science, Griffith University, Nathan, Australia

<sup>4</sup>School of Science, Technology and Engineering, University of the Sunshine Coast, Petrie, Australia

<sup>5</sup>Earth and Planetary Science, McGill University, Montreal, QC, Canada

## Key Points:

- Despite their vast surface area, the High Seas provide only a small fraction of global wild fish catch.
- Dispersion of trophic energy throughout deep water columns and micronutrient limitations leads to smaller fish biomass density in High Seas.
- Smaller biomass density is a major contributor to the small catch; while migration should also matter, economic factors are likely secondary.

---

Corresponding author: Jerome Guet, [jerome.c.guet@gmail.com](mailto:jerome.c.guet@gmail.com)

## Abstract

The High Seas, lying beyond the boundaries of nations' Exclusive Economic Zones, cover the majority of the ocean surface and host roughly two thirds of marine primary production. Yet, only a small fraction of global wild fish catch comes from the High Seas, despite intensifying industrial fishing efforts. The surprisingly small fish catch could reflect economic features of the High Seas - such as the difficulty and cost of fishing in remote parts of the ocean surface - or ecological features resulting in a small biomass of fish relative to primary production. We use the coupled biological-economic model BOATS to estimate contributing factors, comparing observed catches with simulations where: (i) fishing cost depends on distance from shore and seafloor depth; (ii) catchability depends on seafloor depth or vertical habitat extent; (iii) regions with micronutrient limitation have reduced biomass production; (iv) the trophic transfer of energy from primary production to demersal food webs depends on depth; and (v) High Seas biomass migrates to coastal regions. Our results suggest that the most important features are ecological: demersal fish communities receive a large proportion of primary production in shallow waters, but very little in deep waters due to respiration by small organisms throughout the water column. Other factors play a secondary role, with migrations having a potentially large but uncertain role, and economic factors having the smallest effects. Our results stress the importance of properly representing the High Seas biomass in future fisheries projections, and clarify their limited role in global food provision.

## 1 Introduction

The UN High Seas Treaty, agreed upon in March 2023, has been welcomed as an unprecedented step towards protecting the biodiversity of the global ocean (UN General Assembly, 2023). Known as the Biodiversity Beyond National Jurisdiction treaty, it explicitly calls for an integrated ecosystem approach in order to maintain and restore biodiversity and carbon cycle functioning within the 60% of the ocean area that lies beyond nationally-managed Exclusive Economic Zones (EEZs). A fundamental metric of the biodiversity that the treaty aims to protect is the abundance or biomass of marine organisms. However, because of the inaccessibility of the High Seas, and the fact that they falls outside the purview of national research organizations, the biomass of animals in the High Seas is relatively poorly evaluated.

The oceans are thought to harbour most of the remaining wild animal life on the planet (Bar-On et al., 2018). Since the High Seas cover the majority of the ocean surface, one could expect them to host a large fraction of marine life. Consistent with this expectation, roughly 67% of marine primary production is estimated to occur in the vast domain of the High Seas, even though the rate of primary production per unit area is higher in the shallow coastal waters that ring the continents (Behrenfeld & Falkowski, 1997; Carr et al., 2006; Marra et al., 2007). Given that roughly half of global primary production is marine, this implies that one third of all primary production on Earth occurs in the High Seas. Yet, the most comprehensive sampling of marine animals by humans - industrial fishing - recovers only a small fish catch from the High Seas, despite intensifying efforts (Rousseau et al., 2019). In fact, humans only retrieve about a twen-

60 tieth of the global wild fish capture – less than 0.1% of total human caloric supply – from  
61 the High Seas that cover more than half the planet (Schiller et al., 2018). We are not  
62 aware of a widely-recognized explanation for the fact that the High Seas provide so lit-  
63 tle human food.

64 On one hand, the surprisingly small High Seas catch could be explained by economic  
65 and technological constraints. Fuel and time expenditures required to travel long dis-  
66 tances, greater capital requirements for High Seas vessels, or the difficulty of catching  
67 fish in deep waters could result in higher costs of fishing the High Seas (Lam et al., 2011;  
68 Sala et al., 2018). Economic constraints can be further modulated by the variable catch-  
69 ability of the fish resource that is influenced by habitat features such as topography, or  
70 vary between gears targeting pelagic or demersal species (Palomares & Pauly, 2019; Kerry  
71 et al., 2022). On the other hand, the small fish catch relative to primary production could  
72 be a result of ecological features of the High Seas. It is possible that the High Seas have  
73 less efficient transfer of energy from primary production to fish types of commercial in-  
74 terest compared to coastal systems (Eddy et al., 2020), or that primary production in  
75 the High Seas is consumed by fish that periodically migrate to the coastal zone, lead-  
76 ing to spatial redistribution of the biomass of upper trophic levels (Block et al., 2011;  
77 Sumaila et al., 2015). To our knowledge, these alternatives have not been investigated  
78 in a consistent, integrated framework.

79 In recent years, a new generation of numerical marine ecosystem models offers a  
80 novel means to address the chronic undersampling of the High Seas. These models do  
81 not attempt to resolve individual species, but instead use fundamental empirical ecolog-  
82 ical processes to predict the growth and life history of generalized fish communities from  
83 features of the environment, including water temperature and resources from lower trophic  
84 levels, such as primary production and zooplankton biomass (Maury, 2010; Guiet et al.,  
85 2016; Blanchard et al., 2017; Tittensor et al., 2018; Heneghan et al., 2021). While these  
86 models have been designed and parameterized based on the rich observational datasets  
87 available for coastal fisheries (RAM Legacy Stock Assessment Database, 2020; Watson,  
88 2017; Pauly et al., 2020), it is possible to use their ecological principles to make predic-  
89 tions for fish production and biomass in the High Seas.

90 Figure 1 shows predictions from the Fisheries and Ecosystem Model Intercompar-  
91 ison Project (FishMIP) ensemble (Tittensor et al., 2018, 2021) for the High Seas (HS)  
92 compared to coastal seas (CS). All of them estimate a fraction of High Seas biomass,  $B$ ,  
93 relative to the global ocean surface area and primary production in the High Seas: around  
94 60% in the 1990s, the decade when global fish catches peaked (FishMIP bar in Fig. 1a,  
95 see also Appendix A to compare models). Among these models, the BOATS model sim-  
96 ulates fish catches,  $C$ , in addition to biomass by including a coupled economic module  
97 that allocates fishing effort dynamically based on the profitability of fishing at a given  
98 time in the global ocean (Carozza et al., 2016, 2017). BOATS predicts that the HS frac-  
99 tion of catch is less than that of biomass, but nonetheless far above observations at 35%  
100 of global catches in the 1990s (in blue in Fig. 1a). Furthermore, the model incorrectly  
101 simulates substantial growth in the High Seas catch and biomass fractions since 1950 (deep  
102 and light blue lines in Fig. 1b). However, both the initial High Seas catch ratio and its

103 rate of increase in BOATS greatly exceeds observations (black lines in Fig. 1a,b; catch  
104 reconstruction by Pauly et al., 2020, dashed line, and Watson, 2017, dotted line).

105 Here, we use the BOATS model and implemented new processes to test five hypothe-  
106 ses that could contribute to the discrepancies between observed and modeled High Seas  
107 catches, indirectly shedding light on the global commercial biomass distribution (see Ta-  
108 ble 1). The first two hypothesis are economic, testing the degree to which lower profitabil-  
109 ity of High Seas fishing can reasonably explain the low catches (Lam et al., 2011; Palo-  
110 mares & Pauly, 2019). The inherently higher cost involved with travelling to the deep  
111 sea, and operating gear in deep waters is explored through the hypothesis HIGHCOST.  
112 It is also conceivable that a greater dispersal of fish in the vast and deep high-seas makes  
113 it more difficult to catch the existing biomass, tested in hypothesis UNCATCHABLE.  
114 Three additional hypotheses focus on ecological reasons why there may be less biomass  
115 available in the High Seas than would be expected from primary production and water  
116 temperature alone. The limitation of phytoplankton growth because of iron limitation  
117 in high-nutrient low-chlorophyll (HNLC) regions is widely recognized (Moore et al., 2013;  
118 Tagliabue et al., 2017). While micronutrient limitation of higher trophic levels, includ-  
119 ing fish, remains unclear, multiple lines of evidence suggest that iron limitation could also  
120 retard or prevent growth of fish in the High Seas (Galbraith et al., 2019). This is cap-  
121 tured in the IRONLIM hypothesis. The ENERGOPATHS hypothesis distinguishes be-  
122 tween pelagic and benthic energy pathways, to test the possibility that deep waters pro-  
123 duce little fish biomass because the energy of primary production is dissipated in the wa-  
124 ter column before reaching benthic communities, and preferentially routed to small or-  
125 ganisms (Stock et al., 2017; van Denderen et al., 2018). Finally, the MIGRATION hy-  
126 pothesis explores the possibility that seasonal migrations deplete the High Seas of biomass  
127 by bringing “straddling” stocks into coastal waters, where they are more accessible to  
128 fishers. Straddling species represent a significant fraction of total catches (White & Costello,  
129 2014; Sumaila et al., 2015), but the fraction of biomass of these catches produced in the  
130 High Seas is unknown.

**Table 1.** List of hypotheses tested to explain the observed low High Seas vs. coastal catches and their expected effect on key variables, cost, catchability and biomass (see details Material and Methods).

Hypothesis	Cost (c)	Catchability (q)	Biomass (f)
HIGHCOST ( $S_{cost}$ )	↑ with distance/depth	-	-
UNCATCHABLE ( $S_{catch}$ )	-	↓ with depth	-
IRONLIM ( $S_{iron}$ )	-	-	↓ in HNLC regions
MIGRATION ( $S_{mig}$ )	-	-	↓ in HS, ↑ in CS
ENERGOPATHS ( $S_{ener}$ )	-	-	↓ with depth

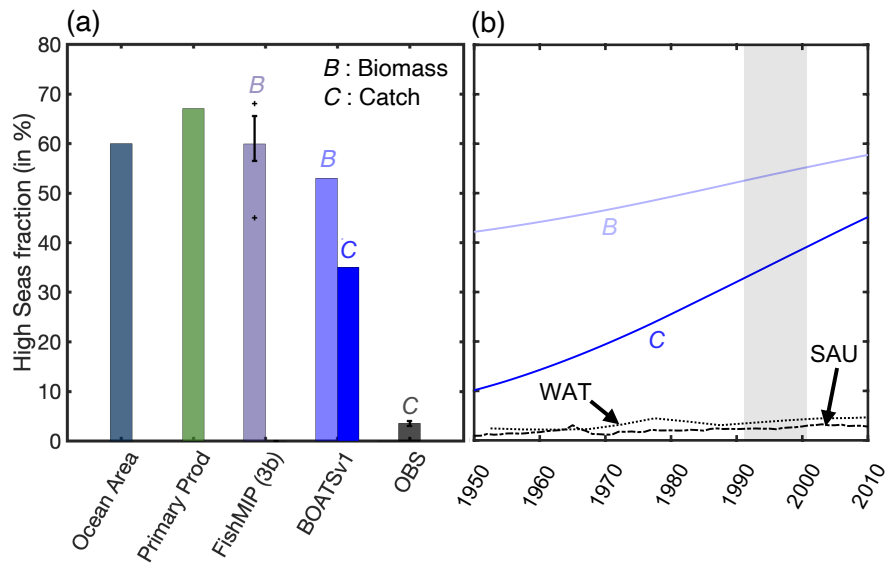


**Figure 1.** Contribution of the High Seas to the global total. (a) The High Seas fraction (%) of global ocean surface area, primary production, simulated biomass  $B$  and catch  $C$ , in the 1990s for 8 models of the FishMIP ensemble (APECOSM, DBPM, EcoOcean, EcoTroph, FEISTY, Macroecological, ZooMSS), BOATSv1, and observed catch (OBS). (b) Historical evolution of biomass,  $B$ , and catch,  $C$ , for BOATSv1 and observations. Observations are based on catch reconstructions from the Sea Around Us (SAU, dashed, Pauly et al., 2020) and Watson (2017) (WAT, dotted). The gray shading panel (b) indicates the time period used for comparisons in panel (a) and Figure 2.

## 2 Material and Methods

### 2.1 Mechanistic modeling framework

To test our hypotheses (Table 1), we use the coupled ecological-economic global marine ecosystem model BOATS to predict fish biomass and catches in the High Seas and coastal waters from environmental and economic drivers (Carozza et al., 2016, 2017). We conducted this analysis using the original BOATSV1 model and an updated version that incorporates several new features, referred to as BOATSV2 (Guet et al., 2024).

BOATS simulates the dynamics of commercial fish biomass, dependent on available resources at the base of the food web. Mean water temperature modulates the rate of biomass propagation across food webs, including production and losses. BOATS is dynamically coupled with an open-access economic module that allow simulations of fishing effort and catch dynamics. Previous work with BOATSV1 showed that the model, forced with globally homogeneous fishing costs and catchability, is able to reproduce the historical development of fisheries when driven by a uniform technological creep (3 to 8% per year, Galbraith, Carozza, & Bianchi, 2017; Guet, Galbraith, Bianchi, & Cheung, 2020). In the following sections, we discuss a series of modifications of BOATSV1 and new simulations aimed at examining our five key hypotheses.

#### 2.1.1 HIGHCOST

In BOATSV1, the cost per unit effort ( $c$ , in  $\$/W/yr$ ) is globally uniform by default. The absence of spatial dependence of cost disregards the importance of transit distance between fishing grounds and ports (Sala et al., 2018), which might be particularly relevant when comparing High Seas and coastal catches. In addition, costs are expected to rise when targeting increasingly deep fishing grounds, due to depth-dependent expenses associated with setting and hauling gears. Since demersal catches account for a large fraction of global catches, this might contribute to the delayed development of High Seas catches as deeper offshore habitats might become profitable later in time (Watson & Morato, 2013). We test both types of variable cost distributions independently under the HIGHCOST hypothesis.

For implementation, we assume that the fishing cost per unit effort is constant in coastal or shallow regions ( $c = c_{CS}$ ). Beyond these regions, the cost increases linearly, either as a function of distance to the nearest shore ( $d_{coast}$ , in  $km$ ), or as a function of seafloor depth ( $z_{bot}$ , in  $m$ ):

$$c(x = d_{coast}, z_{bot}) = \begin{cases} c_{CS} & \text{when } x \leq x^* \\ c_{CS} + \delta_c(x - x^*) & \text{when } x > x^* \end{cases} \quad (1)$$

where  $x$  represents either  $d_{coast}$  or  $z_{bot}$ ,  $x^*$  is a reference value that indirectly determines the boundary of coastal regions, and  $\delta_c$  is a parameter controlling the rate of increase of costs beyond coastal regions (in  $\$/km/W/yr$  or  $\$/m/W/yr$ , for distance to coast or bottom, respectively). We note that calculating distance to the nearest shore to mod-

167 ulate costs is a simplification, particularly for industrial fisheries. We test multiple sets  
 168 of parameters  $[x^*, \delta_c]$  (see Appendix B).

### 169 **2.1.2 UNCATCHABLE**

170 Catchability ( $q$ , in  $m^2/W/yr$ ) refers to the capturability of fish biomass per unit  
 171 effort given fish behavior (e.g. schooling, gear avoidance) and the level of technology, in-  
 172 cluding fishing gear, navigation technologies, sonar, communications and skipper knowl-  
 173 edge. Catchability generally grows exponentially over time through technological progress  
 174 (Palomares & Pauly, 2019; Eigaard et al., 2014), thus driving the historical development  
 175 of fisheries (Galbraith et al., 2017). However, the globally uniform catchability increase  
 176 in BOATSv1 does not account for geographical variations in the marine environment,  
 177 which could be significant. For example, pelagic fish in regions with vertically compressed  
 178 euphotic zones might be more accessible to purse seines than in regions where produc-  
 179 tion is spread over a larger, more diffuse vertical range (Nuno et al., 2022). Under the  
 180 UNCATCHABLE hypothesis, we incorporate spatially varying catchability to assess how  
 181 this might affect catches.

182 First, we test the scenario in which catchability varies as a function of the euphotic  
 183 layer depth ( $z_{eu}$ , in  $m$ ). Second, we test the scenario in which catchability varies as a  
 184 function of seafloor depth ( $z_{bot}$ , in  $m$ ), based on the notion that shallower regions, such  
 185 as those around seamounts or on continental shelves, promote biomass aggregation (Kvile  
 186 et al., 2014) and enhance fisheries' access to marine fish stocks (Kerry et al., 2022). The  
 187 UNCATCHABLE hypothesis tests both variable catchability distributions:

$$q(x = z_{eu}, 1/z_{eu}, z_{bot}, 1/z_{bot}, \log_{10}(z_{bot})) = q_{ref} \left[ q_{min} + (1 - q_{min}) \frac{x_{max} - x}{x_{max} - \bar{x}} \right] \quad (2)$$

188 Here  $x$  represents a function of either euphotic zone or seafloor depth,  $x_{max}$  the global  
 189 maximum of the quantity,  $\bar{x}$  the global mean, and  $q_{min}$  is a parameter that controls the  
 190 change of catchability as a function of depth. Note that we test formulations in which  
 191 catchability decreases either linearly or in proportion to the inverse of either the euphotic  
 192 zone depth or the seafloor depth (see Appendix C). In each formulation, we select  $q_{min}$   
 193 values that provide realistic spatial variations, and use  $5 \times q_{min}$  as an upper bound to catch-  
 194 ability, effectively limiting its variation to the observed range (Palomares & Pauly, 2019).  
 195 The formulation in Equation 2 modulates the global reference catchability ( $q_{ref}$ ), which  
 196 increases annually at 5% rate.

### 197 **2.1.3 IRONLIM**

198 To assess the influence of iron limitation on fish growth, we modulate the trophic  
 199 efficiency  $\alpha$ , a key parameter of BOATS that represents the fraction of organic matter  
 200 incorporated into new tissue at each trophic step:

$$\alpha = \alpha_0 \frac{k_{NO_3^-}}{k_{NO_3^-} + NO_3^-} \quad (3)$$

201 where surface nitrate concentrations ( $NO_3^-$ , in  $\mu M$ ) are taken as a proxy for low iron  
 202 conditions (Moore et al., 2013). Assuming a constant  $k_{NO_3^-} = 5 \mu M$ , this formulation  
 203 smoothly decreases the trophic efficiency relative to the reference value  $\alpha_0$  as nitrate in-  
 204 creases (Galbraith et al., 2019).

#### 205 **2.1.4 ENERGYPATH**

206 BOATSv1 calculates fish biomass from vertically integrated net primary produc-  
 207 tion ( $NPP$ ) and upper water column temperature ( $T_{75}$ ). These quantities determine fish  
 208 growth rates, and ultimately biomass accumulation, in a region. While these forcings are  
 209 relevant for pelagic species, they do not account for the flux of organic material that reaches  
 210 the seafloor as sinking particles, and sets the production of deep-sea ecosystems and fish-  
 211 eries (Blanchard et al., 2011; Stock et al., 2017; Petrik et al., 2019). Moreover, cooler tem-  
 212 peratures at the ocean bottom ( $T_{bot} < T_{75}$ ) result in slower metabolism and produc-  
 213 tion rates for deep-sea species. Both factors – organic material flux and bottom temper-  
 214 ature – must influence new fish biomass production in shallow vs. deep waters. To test  
 215 the effect of distinct drivers of production in pelagic and demersal communities, under  
 216 the ENERGYPATH hypothesis we expand BOATSv1 to provide a separate representa-  
 217 tion of pelagic species, forced by  $NPP$  and  $T_{75}$ , and demersal species, forced by the par-  
 218 ticle flux at the bottom ( $PFB$ ) and  $T_{bot}$ .

219 We derive the  $PFB$  from surface  $NPP$  (Guet et al., 2024), assuming a typical power-  
 220 law attenuation of the particle flux below the euphotic zone ( $z_{euph}$ ):

$$PFB = NPP \cdot pe_{ratio} \cdot \left(\frac{z_{bot}}{z_{euph}}\right)^{b_a} \quad (4)$$

221 where  $b_a = -0.8$  is the coefficient of attenuation of particle fluxes with depth (Martin  
 222 et al., 1987) and  $z_{euph} = 75m$  the average euphotic zone depth, which, for simplicity,  
 223 we keep constant. The term  $(z_{bot}/z_{euph})^{b_a}$  is computed first at a high resolution, using  
 224  $z_{bot}$  values from the global topographic dataset ETOPO 1/10° (Amante & Eakins, 2009),  
 225 and then averaged across each 1° grid cells of the model. Note that when  $z_{bot}$  is shal-  
 226 lower than  $z_{euph} = 75m$ , the seafloor depth is set to be equal to the euphotic zone depth.  
 227 The particle export at the base of the euphotic zone is determined by an empirical es-  
 228 timate of the particle export ratio ( $pe_{ratio}$ ), as a function of local surface temperature  
 229  $T_{75}$  and  $NPP$ , following prior work (Dunne et al., 2005).

#### 230 **2.1.5 MIGRATION**

231 At the coarse resolution of the BOATS model (1°), the horizontal transport of biomass  
 232 by currents and active movement can be assumed to play a secondary role relative to lo-  
 233 cal biomass production for many fish. However, global catches include a significant frac-  
 234 tion of straddling species that can travel large distances (Sumaila et al., 2015). While  
 235 straddling stocks are caught almost exclusively in coastal waters, some fraction of this  
 236 biomass is produced from trophic energy foraged in the High Seas. Fish migration and  
 237 subsequent capture in coastal seas therefore represents a flux of trophic energy from the  
 238 high seas to coastal waters that is not resolved by BOATS. This biomass flux could con-

239 tribute to the discrepancy between modelled and observed catches in the High Seas vs.  
240 coastal regions.

241 Unfortunately, the considerable uncertainty in behavioural drivers of fish migra-  
242 tion prevents an explicit representation of this biomass redistribution at this time. Thus,  
243 unlike the mechanisms described above, we do not include migration as a mechanistic  
244 component of the model. Instead, we gauge the effect of fish migrations by estimating  
245 a plausible contribution of High Sea biomass to the total catch in each EEZ  $i$ , based on  
246 the simulated catch ( $C_i$ ) inside the EEZ, and the fraction of total catch in the EEZ that  
247 can be attributed to straddling species ( $\alpha_{str,i}$ ), which we estimate based on observational  
248 catch reconstructions (see Appendix D):

$$C_i = C_i^{adj} - \delta_s \alpha_{str,i} C_i^{adj} \quad (5)$$

249 where  $C_i^{adj}$  is the total catch adjusted for straddling species in a given EEZ, and the ar-  
250 bitrary factor  $\delta_s$  represents the proportion of the catch of straddling species coming from  
251 the High Seas. This factor provides an indirect measure of the coastal catch contribu-  
252 tion by fish biomass produced in the High Seas. Rearranging terms in Equation 5 pro-  
253 vides an estimate of the total catch  $C_i^{adj}$  from simulated catch within each EEZ  $C_i$ :

$$C_{CS}^{adj} = \sum_{EEZ_s} C_i^{adj} \quad (6)$$

$$C_{HS}^{adj} = C_{HS} - \sum_{EEZ_s} (C_i^{adj} - C_i). \quad (7)$$

254 Ultimately, we use  $C_{CS}^{adj}$  and  $C_{HS}^{adj}$  as updated coastal and High Seas catches after biomass  
255 redistribution by migration of straddling species, as long as  $C_{HS}^{adj} > 0$ . Given that  $\delta_s$   
256 is undetermined, we use a range of values to estimate the magnitude of biomass trans-  
257 fer, and add the resulting High Seas-derived straddling catch to the Coastal Catch.

## 258 2.2 Simulations

259 Our five hypotheses (Table 1) are tested with new simulations compared to the ref-  
260 erence simulation made with BOATSv1 (shown in blue in Fig. 1, hereafter simulation  
261  $S_{v1}$ ). In order to capture uncertainty in model parameters, we run each experiment with  
262 a small ensemble of 5 different parameter sets (Carozza et al., 2017). We take the en-  
263 semble mean as the final result, and when relevant use the spread across the 5 members  
264 as a measure of uncertainty.

265 We first compare means and uncertainties for new simulations that update the ref-  
266 erence model to include economic constraints ( $S_{cost}$  and  $S_{catch}$ , Table 1). Second, we com-  
267 pare new simulations that test the influence of ecological features ( $S_{iron}$  and  $S_{ener}$ ). Be-  
268 cause simulation  $S_{ener}$  changes the structure of the ecological model, we generated 5 new  
269 parameter sets by running a new optimization with a Monte-Carlo ensemble using the  
270 BOATSv2 code (Guet et al., 2024). Similar to the BOATSv1 parameter ensemble, the  
271 BOATSv2 parameter sets were selected to best capture global observations including the  
272 catch peak aggregated by Large Marine Ecosystems (LMEs), and the spatial variabil-

273 ity of historical catch maxima in each LME. BOATSv1 and v2 are both tuned based on  
 274 similar coastal observations, resulting in comparable dynamics in coastal seas. However,  
 275 they markedly differ in their representation of the High Seas. Finally, we evaluate the  
 276 role of straddling species by adjusting catch *a posteriori* from the reference simulation  
 277 ( $S_{mig}$ ).

278 Simulations are run on a  $1^\circ$  global grid, forced with climatological observations of  
 279 the surface mean temperature between 0 and 75m ( $T_{75}$ ) and the temperature near the  
 280 seafloor ( $T_{bot}$ ) from the World Ocean Atlas (Locarnini et al., 2006). We estimated  $T_{bot}$   
 281 as the mean temperature in the water column weighted by the fraction of each depth in  
 282 a model grid cell as reported by ETOPO  $1/10^\circ$  (Amante & Eakins, 2009). For net pri-  
 283 mary production, we take the average of three satellite-based estimates to capture some  
 284 of the variability inherent to primary production models (Behrenfeld & Falkowski, 1997;  
 285 Carr et al., 2006; Marra et al., 2007). To parameterize iron limitation in HNLC regions  
 286 we take the monthly minimum surface nitrate in the World Ocean Atlas climatology (Locarnini  
 287 et al., 2006).

### 288 2.3 Observational constraints

289 To evaluate our hypotheses against observations, we use two spatially explicit re-  
 290 constructions of global catches: SAU, the Sea Around Us from Pauly et al. (2020); WAT,  
 291 from Watson (2017). Both provide global catches at  $1^\circ$  resolution from 1950 to 2014, and  
 292 are corrected for unreported catches. We focus on the following two indicators:

- 293 • (i) The fraction of catch occurring in the High Seas relative to the total catch. We  
 294 compare this ratio around the global catch peak of the 1990s ( $\pm 5$  years around  
 295 1996, gray shading in Fig. 1), for which observations suggest a mean value of 3-  
 296 4% (*OBS* in Fig. 1a). For each simulation, we average the 11 years of catch around  
 297 the peak of catch summed across EEZ, and report the mean and spread (10th to  
 298 90th percentiles) of the 5 ensemble members.
- 299 • (ii) The historical deepening of the global catch. The deepening of catches over  
 300 time serves as an indicator of the rate at which fisheries develop in deep vs. shal-  
 301 low regions. The mean observed seafloor depth weighted by the local catch in the  
 302 1990s is 372m in SAU and 154m in WAT. We compare these estimates with the  
 303 mean depth for the 11-year period around the catch peak across EEZs in the model  
 304 simulations, reporting the ensemble mean and spread.

305 Once the relevant hypotheses are identified, we further evaluate their contribution  
 306 to global fisheries' development by independently comparing simulated catches with pelagic  
 307 and demersal catch reconstructions from the SAU (see Appendix E for the definition of  
 308 demersal and pelagic groups). We also compare regional catch variations across LMEs  
 309 and 11 High Seas ecosystems when sequentially including new processes (HSEs, Appendix  
 310 F).

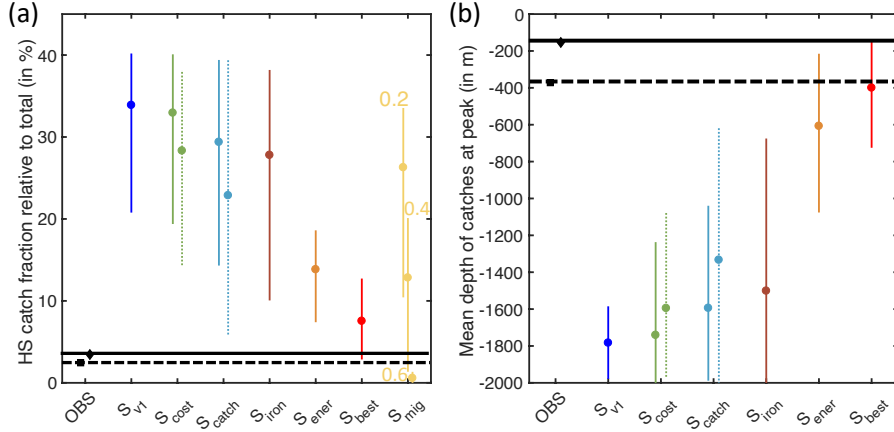


**Figure 2.** Influence of the hypothesized mechanisms (Table 1) on High Seas fisheries development. (a) Observed and simulated High Seas catch fraction. (b) Observed and simulated mean depth of catches. Values reflect the global catch peak of the 1990s. Simulations are compared with reconstructions from the SAU (black squares and dashed horizontal lines, Pauly et al., 2020) and WAT databases (black diamonds and solid horizontal lines, Watson, 2017). Both panels show the model’s ensemble mean and 10-90th percentile range, for each simulation set. In both panels, solid and dotted ranges indicate model variants with distinct parameterizations, i.e., distance- or depth-dependent costs for  $S_{cost}$ , euphotic layer- or seafloor- dependent catchability for  $S_{catch}$ . In panel (a), for  $S_{mig}$ , each range corresponds to a distinct value of the factor  $\delta_s$ , as reported on the figure.

### 3 Results and discussion

#### 3.1 Small effect of economic constraints

Both hypotheses related to economic mechanisms (HIGHCOST and UNCATCHABLE) are unable to correct the excessive High Seas catches of the reference simulation  $S_{v1}$  when keeping realistic parameterizations (see  $S_{cost}$  in green and  $S_{catch}$  in light blue, Fig. 2a). Higher fishing costs in the High Seas within the range of observations (i.e., [6.94-8.87]\$/W/yr, Sala et al. (2018)) only decrease the fraction of High Seas catches to, on average, 29% (from 35%), while delayed development of fisheries in offshore regions for spatially variable catchability (with deeper euphotic zones and bottom depths) decreases the fraction to 23%. Both remain high compared to the observed 3-4% (see Appendices B,C).

The shift of global catches to shallower fishing grounds is also insufficient for both economic hypotheses (Fig. 2b). But, improvements are substantial, especially when applying depth-dependent fishing costs and catchabilities (Appendices B,C). Access to deep demersal stocks or aggregation of pelagic biomass around seamounts and in shallow regions can contribute to the slow deepening of fishing through time.

### 3.2 Large effect of energy pathways

Among hypotheses related to ecological mechanisms (IRONLIM and ENERGY-PATH), iron limitation of fish partially reduces the mean High Seas catch ratio (down to 28% on average, see  $S_{iron}$ , brown line in Fig. 2a). The magnitude is comparable to other economic hypotheses. While allowing the pelagic and demersal communities to develop independently from separate food resources at low trophic levels significantly corrects the fraction (down to 13%, see  $S_{ener}$ , orange line in Fig. 2a). These improvements are consistent with a reduced High Seas catch fraction attributable to lower fish biomass production in the High Seas compared to coastal waters.

Similar to other economic constraints, with iron limitation the mean depth of catch remains much deeper than observed (brown line in Fig. 2b). Iron limitation might influence biomass production and thus fisheries yields in the High Seas, yet a link with seafloor depth is lacking. In contrast, having independent pelagic and demersal communities allows a more abundant demersal biomass in shallow waters, which support larger coastal fisheries and ultimately reduces the historical deepening of global catches (orange line in Fig. 2b). Our simulations of the ENERGYPATH hypothesis indicate that it is a fundamental mechanism leading to relatively low catches in the High Seas.

### 3.3 Combined economic and ecological effects

Taken in isolation, ecological features limiting biomass production in High Seas best explain the smaller High Sea catches (IRONLIM and ENERGYPATH), while economic constraints are insufficient (HIGHCOST and UNCATCHABLE). However, the inclusion of economic constraints could still influence spatio-temporal dynamics.

Historically, observed demersal catches are largely coastal (60 times larger inside EEZ than High Seas in 2000s, compare black solid and dotted lines in Fig. 3a), while pelagic catches are more evenly distributed between coastal waters and the High Seas (20 to 1 in 2000s, Fig. 3b). When the ecological features are implemented in BOATS, they largely capture the historical variation of catch for each functional type, with slight overestimation of High Seas catches (orange lines in Fig. 3). Yet, development of High Seas fisheries still occurs in the model and becomes increasingly over-estimated after 1990. The selected economic constraints mitigate this bias by reducing catch on the more homogeneously distributed pelagic biomass (red lines in Fig. 3). For instance, with depth-dependent demersal fishing costs and depth-dependent pelagic catchabilities, the fraction of High Seas catch reaches 8% for a mean depth of catch of 400m, close to observation (see  $S_{best}$  Fig. 2).

Spatially (Fig. 4), the addition of ecological features corrects the simulated catch densities across LMEs and HSEs (from  $R=0.73$  to  $0.83$ , while RMSE is halved, Figs. 4a,b). The correction is especially important in regions over deeper seafloors (compare color shadings in Figs. 4a,b). In shallower coastal regions, yields remain comparable, as pelagic and demersal communities experience similar environmental forcing (compare circles in Figs. 4a,b). In deeper regions, especially in the High Seas, yields drop markedly, in agreement with a lower biomass production (compare darker markers and triangles). Economic

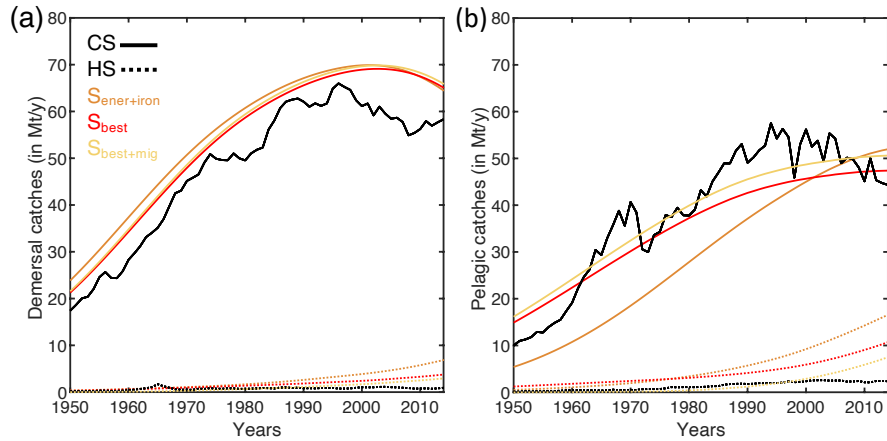


**Figure 3.** Historical evolution of pelagic and demersal catch. (a) Historical demersal fish catch. (b) Historical pelagic fish catch. In each panel, the solid lines indicate catches inside EEZs, while dotted lines indicate catches in the High Seas. Simulations including ecological corrections ( $S_{ener+iron}$  in orange), ecological and economic corrections ( $S_{best}$  in red), and correction for straddling biomass ( $S_{best+mig}$  in yellow).

368 features have a smaller effect (correlation from  $R=0.83$  to  $0.84$ , RMSE decreases from  
 369  $0.16$  to  $0.11$ , Figs. 4b,c). The influence of depth on costs and catchability further delays  
 370 the development of fisheries in High Seas, ultimately reducing yields at the peak in the  
 371 1990s (compare triangles in Figs. 4b,c). Economic constraints must have impacted the  
 372 development of High Seas fisheries, yet their effect on the small High Seas catch fraction  
 373 is secondary compared to the mechanisms that govern the global fish biomass distribu-  
 374 tion.

375 Together, the selected economic and ecological hypotheses explain the variability  
 376 of global catch with high fidelity (compare spatial distributions in the 1990s, Figs. 4d  
 377 and e). Notable mismatches remain in the Western Equatorial Pacific, which supports  
 378 larger fisheries than simulated by the model, and in Arctic waters, where the model over-  
 379 estimates catches. Our definition of economic constraints could influence the mismatches,  
 380 or these indicate missing processes. New observational metrics will be necessary to weigh  
 381 the effect of these mechanisms. While fisheries management must also influence regional  
 382 dynamics (K. Scherrer & Galbraith, 2020), smaller High Seas catches primarily results  
 383 from lower biomass densities in these regions.

### 384 3.4 Migration redistributes biomass

385 Thus far, we have not addressed the role of migrating fish biomass from High Seas  
 386 to the coast. Our analysis shows that straddling species, migrating between coastal wa-  
 387 ters and the High Seas, are caught in many high latitude and subtropical insular EEZs,  
 388 where they often contribute more than 80% of local catches (see Appendix D). This could  
 389 represent a large biomass transfer from the High Seas to the coast, if the fish are ener-  
 390 getically supported by High Seas primary production through a significant part of their

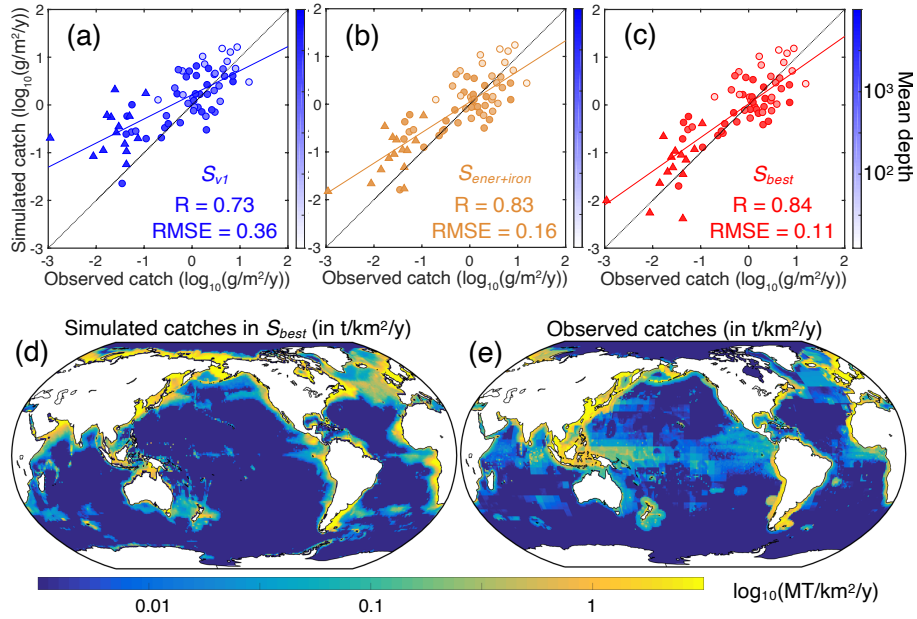


**Figure 4.** Regional catch variation at the global peak in the 1990s. Observed vs. simulated mean catch densities by regions of the global ocean for: (a) the reference simulations  $S_{v1}$ ; (b) simulations including ecological features that limit production in the High Seas (HS)  $S_{ener+iron}$ ; (c) simulations including ecological features and economic constraints  $S_{best}$ . (d) Map of simulated global catches at peak for the best simulations including ecological and economic features influencing catch in the HS, at global peak. (e) Map of observed global catches at peak. Panel (a-c), the circular markers indicates LMEs, the triangles HSEs (see Appendix F), the lines show linear fits across data, and the shadings indicate variations in the mean depth of each region, on a log<sub>10</sub> scale (in  $m$ ).

391 life cycle. Assuming that, for example, 50% of straddling catch is derived from High Sea  
 392 production (i.e., 40% of total catch, where 80% of the catch is straddling) would bring  
 393 the modelled High Seas to coastal seas catch ratio closer to observations (see  $S_{mig}$  Fig. 2a,  
 394 yellow line). However, to maintain realistic High Seas catches (i.e., about 4  $Mt/y$ ), the  
 395 adjustment of the reference simulation ( $S_{v1}$ ) would require a migration of more than 60%,  
 396 which would imply a catch fraction much smaller than observed ( $1 < \%$ , Fig. 2a). Thus,  
 397 migration could be a very important contributor, but is insufficient alone to explain the  
 398 small catches in the High Seas.

399 This analysis highlights the potential for migration of straddling species to natu-  
 400 rally extract biomass from the High Seas, since, as long as High Seas biomass density  
 401 remains lower than coastal seas, migrating biomass will be caught more profitably in coastal  
 402 regions. When High Seas catches are reduced by lower High Seas biomass (best simu-  
 403 lation,  $S_{best}$ ), correction or remaining discrepancies between the model and observations  
 404 would require setting 5% of demersal and 10% of pelagic coastal catches on straddling  
 405 species to come from the High Seas (compare red and yellow lines in Fig. 3). These val-  
 406 ues modulate the excessive development of High Seas fishing, while allowing realistic High  
 407 Seas catches (4  $Mt/y$ ) and are, therefore, plausible. But migration is hard to constrain,  
 408 and more work is required to link regions of biomass production to biomass extraction  
 409 that goes beyond the scope of this study.

### 410 3.5 Small High Seas fish biomass and implications

411 The small High Seas catch fraction requires that, for the same level of primary pro-  
 412 duction, High Seas produce less biomass of commercially targeted fish (see  $S_{best}$  Fig. 2).  
 413 Based on our results, the dominant mechanism behind this small production is the sep-  
 414 aration of prey resources for pelagic and demersal communities (ENERGYPATH).

415 Both prey resources,  $NPP$  and  $PFB$ , are available at distinct relative abundances  
 416 in High Seas and coastal seas (see  $PFB/NPP$  ratios in Fig. 5a). In coastal seas, dem-  
 417 ersal resources from particle fluxes are on average  $10\times$  less abundant than  $NPP$ . This  
 418 proportion decreases to  $100\times$  less abundant in the High Seas, because of the increased  
 419 dissipation of energy of primary production over deeper water columns. Within each re-  
 420 gion, other mechanisms must compensate for less abundant demersal resources to allow  
 421 comparable pelagic and demersal biomass densities (Fig. 5b), ultimately explaining the  
 422 similar magnitude of demersal and pelagic catches in observations (Fig. 3).

423 A likely candidate mechanism is that, in demersal communities, the processing of  
 424 detritus by large detritivores in benthic ecosystems shortens the length of food chains  
 425 before energy reaches the exploitable demersal fish biomass. In BOATS, food chains are,  
 426 on average, shorter by 1 to 1.4 trophic levels in coastal and High Seas respectively (Fig. 5c).  
 427 For an average trophic efficiency of 0.1, such compensation can correct the factor-of-10  
 428 discrepancy in coastal seas, but is insufficient to correct the factor-of-100 discrepancy  
 429 in High Seas. In summary, shorter demersal food chains support larger demersal biomass  
 430 than pelagic biomass in coastal areas. In the High Seas, a larger proportion of the en-

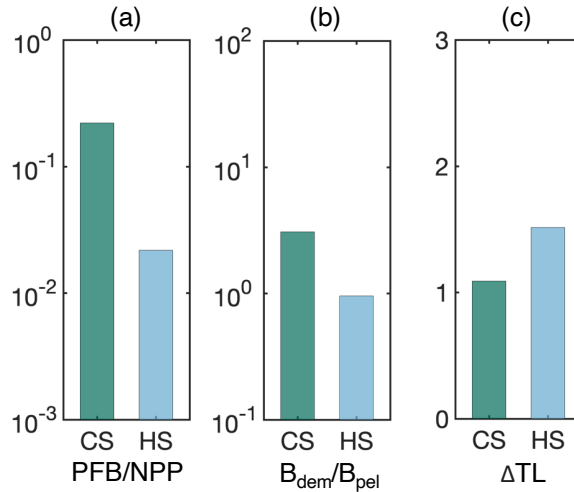


**Figure 5.** Drivers of the difference in pelagic and demersal biomass. (a) Ratio of low trophic level resources ( $PFB/NPP$ ) for demersal vs. pelagic communities. (b) Demersal vs. pelagic biomass ratio ( $B_{dem}/B_{pel}$ ). (c) Trophic distance of fish recruits relative to the representative size of the low trophic level prey. Each unit indicates one additional trophic level for the pelagic community relative to the demersal community. Green and blue bars show coastal (CS) and High Seas (HS) respectively. The ratios are means for the global ocean, weighted by fish biomass and with masked HNLC regions.

431 energy available from photosynthesis is lost, leading to a smaller biomass density per unit  
 432 of  $NPP$ .

433 Our best simulation shows a notable contrast in the change of biomass over time  
 434 between High Seas and coastal waters. In the early 20th century, the total biomass of  
 435 commercially-targeted fish in coastal waters is 1.8 Gt, 2-3 times larger than that of the  
 436 High Seas. The subsequent extraction of commercial fish in coastal regions causes coastal  
 437 biomass to decline to only 0.8 Gt by 2013 (Fig. 6), a rate of decline comparable to a pre-  
 438 vious analysis (Worm & Branch, 2012; Bianchi et al., 2021). As a result, the model sug-  
 439 gests that the High Seas presently harbor a similar amount of biomass as coastal regions,  
 440 but spread over a much larger area, and that the fraction of global fish biomass in the  
 441 High Seas has increased from 30% to 50%. We note that our simulations do not include  
 442 migrations, which would have caused the High Seas biomass to decrease by a larger amount.  
 443 Without effective fisheries management (i.e., under open-access dynamics), economic the-  
 444 ory suggests that fishing will eventually even out the biomass distribution across High  
 445 Seas and coastal regions, and continual increases in price and/or technological progress  
 446 will render previously unprofitable regions suitable for exploitation (compare High Seas  
 447 and coastal seas biomass in Fig. 6).

## 448 4 Conclusion

449 We shed light on why so few fish are caught in the High Seas by testing a suite of  
 450 hypotheses using a global fisheries model constrained by global catch observations. Our

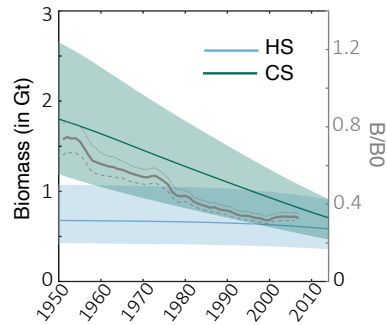


**Figure 6.** Historical evolution of global biomass under fishing. The green and blue colors show coastal and High Seas respectively, the envelopes the 10-90th percentile ranges for each simulation set, and the gray lines the observed change in biomass based on stock assessments (Worm & Branch, 2012).

451 results indicate that the primary factor is simply that the biomass of commercially tar-  
 452 geted fish in the High Seas is small compared to that of coastal waters. This is an im-  
 453 portant insight for global marine ecosystem modeling efforts (Lotze et al., 2019; Titten-  
 454 sor et al., 2021) as many models predict large High Seas biomass fraction (see the mean  
 455 of FishMIP ensemble in Fig. 1a). Our simulations provide ecologically feasible mecha-  
 456 nisms to explain this discrepancy, including the dependence of trophic pathways on wa-  
 457 ter depth, and micronutrient limitation. Economic constraints alone cannot explain the  
 458 low fish catches in the High Seas, but likely modulate the rate of development of High  
 459 Seas fisheries. Finally, migration of straddling species from the High Seas to coastal re-  
 460 gions is difficult to represent and quantify, but is likely to play a significant role in de-  
 461 pleting High Seas fish populations by exposing them to fishing effort in coastal waters.  
 462 In essence, a significant fraction of High Seas fish may be caught when they migrate to  
 463 coastal waters, without the need to fish far from port.

464 We suggest that the most important ecological factor explaining the low High Seas  
 465 catches is the impact of water depth on organic matter consumption (Buesseler & Boyd,  
 466 2009). In coastal seas, the concentration of organic production in a thin layer, with fewer  
 467 trophic steps between primary producers and commercial fish, allows a much larger por-  
 468 tion of the energy to be channeled to the large organisms humans prefer to eat, and sup-  
 469 ports demersal species that dominate on upper shelf slopes (Haedrich & Merrett, 1992;  
 470 Stasko et al., 2016). In the High Seas, the outputs of primary production are volumet-  
 471 rically diluted, and are consequently consumed by microbes and filter feeders over an ex-  
 472 tended vertical range of the water column, without accumulating in sufficiently high den-  
 473 sity to support abundant populations of large fish. Note that mechanisms that couple  
 474 pelagic and demersal communities could modulate this difference, such as vertical mi-  
 475 grations that enable predator-prey interactions across overlapping vertical habitats (Sutton  
 476 et al., 2008; Trueman et al., 2014). The lack of trace nutrients may also contribute to  
 477 the sparsity of the pelagic community, for example the low availability of the essential  
 478 element iron in waters far from shore (Galbraith et al., 2019). As a result, there are fewer

479 commercially valuable fish to be found in the High Seas. We note that small mesopelagic  
480 fish may be abundant in the High Seas, particularly where primary production is ele-  
481 vated (Irigoien et al., 2014; Proud et al., 2018). The relatively high abundances of mesopelagic  
482 fish can be attributed to their ability to intercept dispersed sinking fluxes, and a lower  
483 susceptibility to iron limitation (Le Mézo & Galbraith, 2021). We have not attempted  
484 to explicitly quantify mesopelagic fish here given that they are not commercially exploited  
485 at present and therefore cannot be constrained by catch records, a key part of our method-  
486 ology.

487 Our results support prior work emphasizing that the High Seas cannot provide a  
488 significant amount of wild fish for direct human consumption (Sumaila et al., 2015; Schiller  
489 et al., 2018). Although wild fish are relatively nutrient-rich (Golden et al., 2021; Heilpern  
490 et al., 2021), the rate at which they are produced is small compared to the overall hu-  
491 man food system, which is dominated by terrestrial agriculture (K. J. Scherrer et al., 2023),  
492 and the potential of the High Seas to provide additional food is minimal. This is also  
493 consistent with historical evidence showing that fisheries in the High Seas have decimated  
494 populations of top predators (Cullis-Suzuki & Pauly, 2010; Pacoureau et al., 2021; Juan-  
495 Jordá et al., 2022), altering the size structure of the overall community (Hatton et al.,  
496 2021), despite providing limited food to humans. Instead of food provision, closing the  
497 High Seas to fishing would have the potential benefits of increasing High Seas biodiver-  
498 sity (Gjerde et al., 2016; Sala et al., 2021), reducing fishing gear waste (Helm, 2022), and  
499 eliminating costly subsidies and fuel-inefficient fishing practices (White & Costello, 2014;  
500 Sala et al., 2018). Timely protection of High Seas ecosystems may help buttress them  
501 against increasing pressures to intensify fishing as technological innovations cause them  
502 to become financially more attractive despite their low fish biomass density.

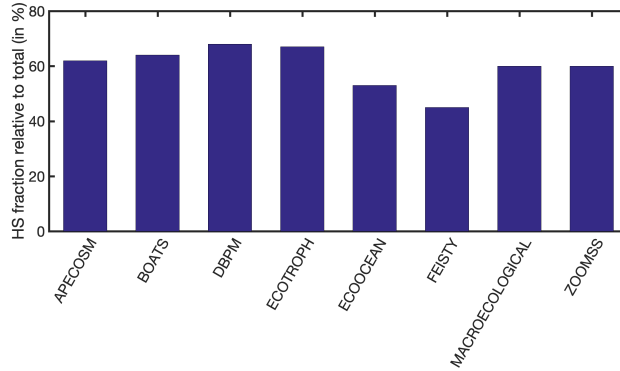


**Figure A1.** Mean contribution of the High Seas biomass to the global total per FishMIP model of the ISIMIP3b simulations forced with IPSL-CM6A-LR (Tittensor et al., 2021).

## 503 Appendix A High seas biomass fraction in FishMIP models

504 Despite large differences in model structure, global fish biomass models suggest a  
505 comparable fraction of High Seas to coastal seas biomass.

## 506 Appendix B Variable fishing costs

507 The cost of fishing varies per fishing gear, per fish community targeted (Lam et al.,  
508 2011). To best constrain spatially variable costs we use estimates of these separate fish-  
509 ing costs in the high-seas (HS) for the main gear types (98% of total effort) following data  
510 reported by Sala et al. (2018). Table B1 summarizes these estimated costs. These com-  
511 pare with BOATS's default fishing cost of  $5.85\$/W/yr$  (Carozza et al., 2017; Galbraith  
512 et al., 2017).

513 Figure B1 summarizes the effect of spatially heterogeneous fishing costs on the ra-  
514 tio HS vs. CS catch, on the variations of the mean depths above which catch occur, as  
515 well as the global mean HS fishing cost, once weighted by effort.

516 First, increasing the cost of fishing with distance to nearest shore [ $x^* = 370, \delta_d$ ]  
517 can partly correct the ratio of catches between HS and CS (Fig. B1a). But most catch  
518 remain over deep seafloor, unlike suggested by observation (mean depth of catch  $\approx 1000$ m  
519 Fig. B1b).

520 Second, increasing the cost of fishing with seafloor depth [ $x^* = 200, \delta_z$ ] can cor-  
521 rect both the ratio of catches between HS and CS, and contributes to the shallowing of  
522 the mean seafloor depth of catches Figs. B1a,b). But, this correction corresponds to un-  
523 realistic high HS fishing costs ( $\approx 8.87\$/W/yr$ , upper range of observed costs Fig. B1c),  
524 inconsistent with observation (Tab. B1).

525 In both cases, spatially variable fishing costs within the range of observation can  
526 not account for the small fraction of HS vs. CS catches. We tested the effect of separate  
527 costs  $\delta_{d,z_{bot}}$ , adjustment of the parameter  $x^*$  only slightly modify the results. For a re-

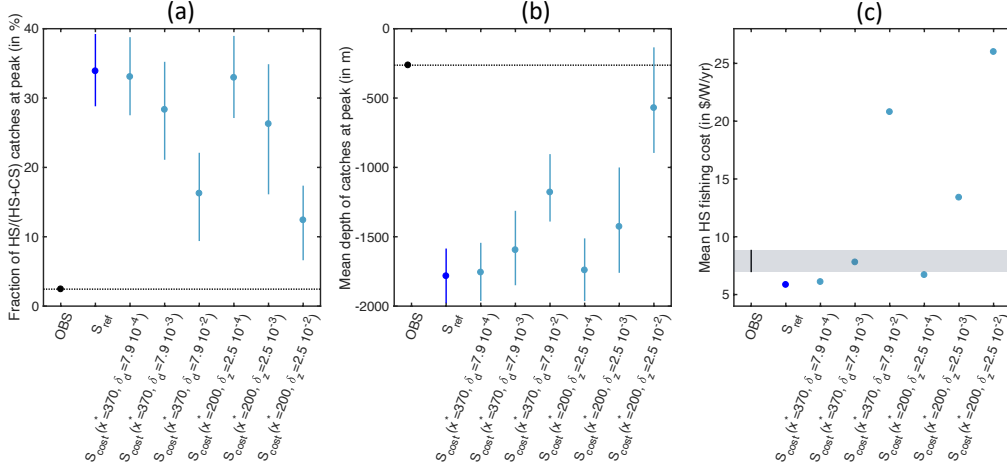


**Figure B1.** Effect of spatially heterogeneous costs. (a) Observed and simulated fraction of HS vs. CS catches at global peak for multiple model variants. (b) Observed and simulated mean depth of catches at global peak for multiple model variants. (c) Observed and simulated mean HS fishing costs once weighted by local fishing effort, around 2010. Panels (a,b) show the ensemble mean as well as the 25-75th percentile ranges per simulation set compared to observation, black dot and horizontal dotted line. Panel (c) shows mean simulated costs and how they compare to the range of observation Tab. B1 (grey shading).

528 alistic cost of fishing the high seas the correction of HS vs. CS ratio seems impossible.  
 529 We conclude that cost alone does not explain the smaller exploitation of the high-seas.

**Table B1.** Cost of fishing the high-seas based on estimates from Sala et al. (2018) for year 2016.

Gear type	Effort in kWh (fraction of total)	Cost range in \$	Cost per unit effort in \$/W/yr
Trawlers	979 10 <sup>6</sup> (15%)	[750 10 <sup>6</sup> -1030 10 <sup>6</sup> ]	[6.7-9.2]
Long liners	3719 10 <sup>6</sup> (55%)	[2523 10 <sup>6</sup> -3023 10 <sup>6</sup> ]	[6.0-7.1]
Purse seiners	394 10 <sup>6</sup> (6%)	[702 10 <sup>6</sup> -1188 10 <sup>6</sup> ]	[15.7-26.0]
Squid jiggers	1490 10 <sup>6</sup> (22%)	[1308 10 <sup>6</sup> -1616 10 <sup>6</sup> ]	[7.7-9.5]
Range all gears	(98%)	-	[6.94-8.87]
BOATS default	-	-	5.85

### Appendix C Variable biomass catchabilities

530  
 531 The catchability of fish biomass per unit effort can vary between species (e.g. school-  
 532 ing or dispersed species), depending on the preferred depth inhabited by these species,  
 533 from the surface to the limit of the euphotic layer depth and to the seafloor. To constrain  
 534 the spatially variable catchabilities, we compare with estimates of the variability of tech-  
 535 nology coefficients per fishing gears as detailed in Palomares and Pauly (2019). Table C1

536 summarizes these estimated coefficients and how they vary. In BOATS the coefficients  
 537 are spatially homogeneous (value of 1) by default.

538 Figure C1 summarizes the effect of spatially variable catchabilities on the ratio HS  
 539 vs. CS catch, and on variations of the mean depths above which catch occur.

540 The spatial variation of catchability as a function of the depth of the euphotic layer  
 541 ( $z_{eu}$ ,  $1/z_{eu}$ ,  $\log_{10}(z_{eu})$ ) or seafloor depth ( $z_{bot}$ ,  $\log_{10}(z_{bot})$ ) only allows a limited redis-  
 542 tribution of catches from the high seas to the coast (Fig. C1a). The mean depth over  
 543 which fishing occurs is also partially corrected with each profile (Fig. C1b).

544 Allowing spatially variable catchabilities while keeping the range within observa-  
 545 tional ranges (Table C1) does not allow correction of the delayed development of high  
 546 seas fisheries compared to coastal ones. We conclude that catchability alone can not ex-  
 547 plain the smaller exploitation of the high-seas. However, slight variations of the catch-  
 548 ability could contribute to explain the overall shallow depth of catch, especially when  
 549 catchability varies with  $\log_{10}(z_{bot})$  (Fig. C1b).

**Table C1.** Technology coefficients per fishing gear based on estimates from Palomares and Pauly (2019) for year 1995 (relative to mean).

Gear type	Technology coefficient
Super trawler	1.19
Freeze trawler	0.95
Stern trawler	0.90
Trawlers	0.86
Shrimp trawler	1.05
Tuna seiner	0.76
Tuna longliner	1.10
Purse seiner	0.95
Longliner	1.33
Gillnetter	0.71
Multipurpose	1.19
Range all gears	[0.71-1.33]
BOATS default	1

## 550 Appendix D Straddling fraction per EEZ

551 The migration of fish biomass can influence the spatial correlation of regions where  
 552 biomass is produced and where it is caught by fisheries. While the straddling fraction  
 553 of catch in an EEZ does not necessarily reflect the fraction of biomass produced outside  
 554 this region, it provides an estimate of the plausible range of redistribution. We inferred  
 555 the straddling catch fraction from Sea Around Us (SAU) reported catch per species within  
 556 each EEZ, separately summing catch on species solely caught inside EEZs ( $C_{EEZ}^{loc}$ ), and  
 557 catch on species caught both in EEZs and highseas ( $C_{EEZ}^{str}$ ,  $\alpha_{str} = C_{EEZ}^{str}/(C_{EEZ}^{str} +$   
 558  $C_{EEZ}^{loc})$ ). We use the list of species in Sumaila et al. (2015) for this distinction. Figure D1a

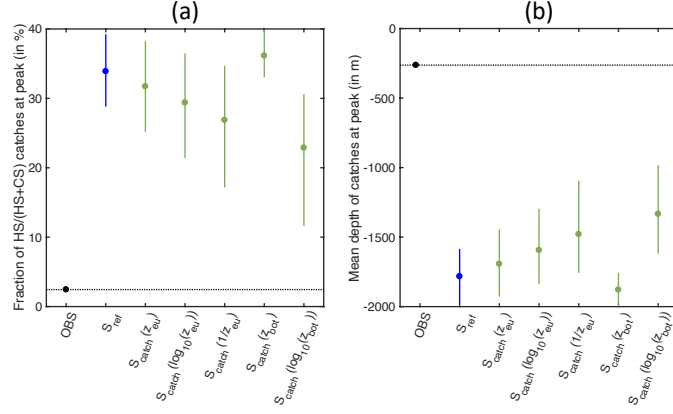


**Figure C1.** Effect of spatially heterogeneous catchabilities. (a) Observed and simulated fraction of HS vs. CS catches at global peak for multiple model variants. (b) Observed and simulated mean depth of catches at global peak for multiple model variants. Panels (a,b) show the ensemble mean as well as the 25-75th percentile ranges per simulation set compared to observation, black dot and horizontal dotted line.

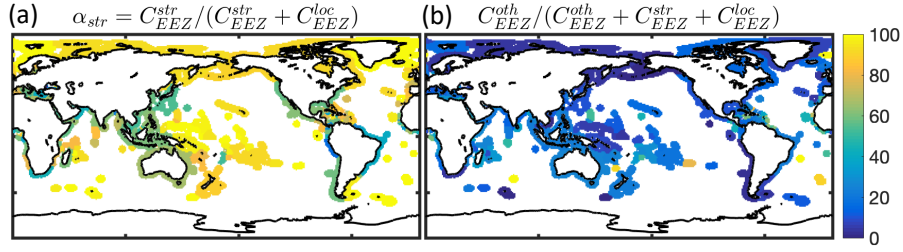


**Figure D1.** Straddling fraction of catches across EEZs during the 1990s (in %). (a) Fraction of catch on straddling species compared to catch on non straddling species  $\alpha_{str}$ . (b) Fraction of catch on species for which the identity is not provided (in %).

559 shows the estimated mean fraction of straddling catch per LME around the global peak  
 560 harvest of the 1990s. Note that for each region, a fraction of catch could not be linked  
 561 to species  $C_{EEZ}^{oth}$ , but this fraction is minimal in most EEZs (see Fig. D1b), and thus dis-  
 562 regarded in our analysis of the straddling catch fraction.

563 Figure D2 summarizes the effect of redistributing an increasing ratio  $\delta_s$  of catch  
 564 from the HS to the CS, in proportion to the fraction of simulated catch on straddling  
 565 species  $\alpha_{str}$  in each EEZ. It also shows the corresponding annual HS catches.

566 Increasing  $\delta_s$  has the expected effect of strongly reducing the HS vs. CS catch frac-  
 567 tion (Fig. D2a), up to matching observation for  $\delta_s = 0.5$ . Despite the improve-  
 568 ment, remain-  
 569 ing catches in the HS are significantly larger than what is observed ( $\sim 4 \cdot 10^6 MT/y$ ,  
 570 observation around peak of the 1990s, see Fig. D2b). We conclude that the biomass re-  
 571 distribution by migrating species alone does not explain the smaller exploitation of the  
 high seas, nevertheless it must have a significant impact.

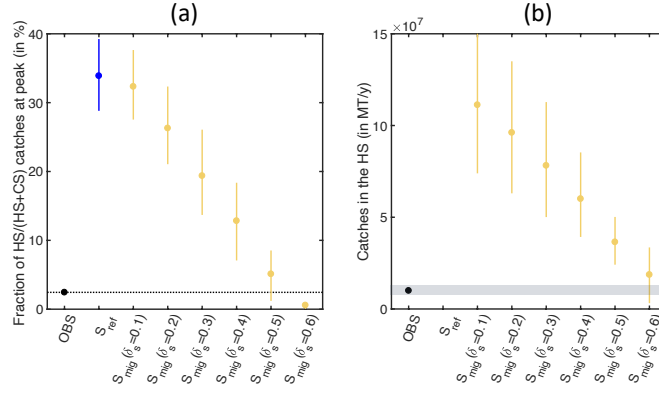


**Figure D2.** Effect of catch redistribution. (a) Observed and simulated fraction of HS vs. CS catches at global peak for multiple model variants. (b) Annual HS catch around the catch peak of the 1990s. Panels (a,b) show the ensemble mean as well as the 25-75th percentile ranges per simulation set compared to observation, black dot and horizontal dotted line.

572 **Appendix E Pelagic and Demersal catches in SAU**

573 We compare simulated pelagic and demersal catches with global catch reconstruction  
 574 from Sea Around Us (SAU) (Pauly et al., 2020). Table E1 lists how we distribute  
 575 the functional types of SAU to generate aggregated maps of pelagic and demersal catches.

**Table E1.** Association of SAU functional types to pelagic and demersal catches.

Catch type	SAU functional types
Pelagic	pelagic s/m/l
	bathypelagic s/m/l
	cephalopods
Demersal	demersal s/m/l
	reef-associated s/m/l
	benthopelagic s/m/l
	bathydemersal s/l
	shark s/l
	flatfish s/l
	ray s/l
	shrimp
	lobster and crab
other demersal invertebrates	

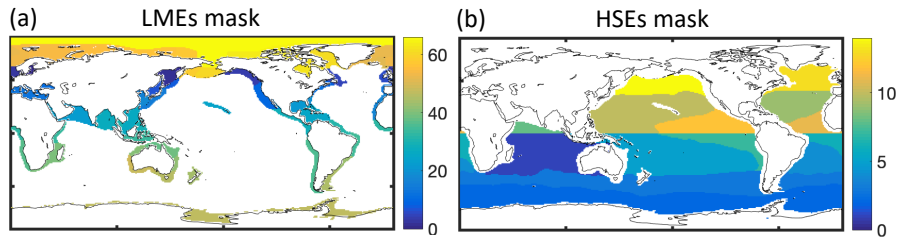


**Figure F1.** Regional masks to compare observation and simulation. (a) Large Marine Ecosystems. (b) High Seas Ecosystems adapted from Weber et al. (2016).

## Appendix F Large Marine Ecosystems and High Seas Ecosystems

Catch are compared across Large Marine Ecosystems (LMEs) for coastal regions, and 11 High Seas Ecosystems (HSEs). Figure F1a, b illustrate respectively the LME and HSE masks.

### Open Research Section

All data and the model used in this study are publicly available. Catch observation used for comparison of simulations can be obtained from the links <https://www.searoundus.org> and <http://dx.doi.org/10.4226/77/58293083b0515>. Biomass simulations from FishMIP can be obtained from the link <https://www.isimip.org/outputdata/>. Other processed data, as well as the code of the model BOATS used for this analysis, are available at the link <https://zenodo.org/records/10662929>.

### Acknowledgments

D.B. and J.G. acknowledge support from the US National Aeronautics and Space Administration (NASA) grant 80NSSC21K0420. Computational resources were provided by the Expanse system at the San Diego Supercomputer Center through allocation TG-OCE170017 from the Advanced Cyber infrastructure Coordination Ecosystem: Services and Support (ACCESS) program, which is supported by National Science Foundation grants 2138259, 2138286, 2138307, 2137603, and 2138296. E.D.G. was supported by the Canada Research Chairs Program fund number CRC-2020-00108. K.J.N.S was supported by the Norwegian Research Council, project 326896.

### References

- Amante, C., & Eakins, B. W. (2009). Etopo1 arc-minute global relief model: procedures, data sources and analysis.
- Bar-On, Y. M., Phillips, R., & Milo, R. (2018). The biomass distribution on earth. *Proceedings of the National Academy of Sciences*, 115(25), 6506–6511.
- Behrenfeld, M. J., & Falkowski, P. G. (1997). Photosynthetic rates derived from satellite-based chlorophyll concentration. *Limnology and Oceanography*, 42(1),

- 603 1–20.
- 604 Bianchi, D., Carozza, D. A., Galbraith, E. D., Quiet, J., & DeVries, T. (2021). Es-  
605 timating global biomass and biogeochemical cycling of marine fish with and  
606 without fishing. *Science advances*, *7*(41), eabd7554.
- 607 Blanchard, J. L., Heneghan, R. F., Everett, J. D., Trebilco, R., & Richardson, A. J.  
608 (2017). From bacteria to whales: Using functional size spectra to model  
609 marine ecosystems. *Trends in Ecology & Evolution*, *32*(3), 174–186. doi:  
610 10.1016/j.tree.2016.12.003
- 611 Blanchard, J. L., Law, R., Castle, M. D., & Jennings, S. (2011). Coupled energy  
612 pathways and the resilience of size-structured food webs. *Theoretical Ecology*,  
613 *4*(3), 289–300. doi: 10.1007/s12080-010-0078-9
- 614 Block, B. A., Jonsen, I. D., Jorgensen, S. J., Winship, A. J., Shaffer, S. A., Bograd,  
615 S. J., ... others (2011). Tracking apex marine predator movements in a  
616 dynamic ocean. *Nature*, *475*(7354), 86.
- 617 Buesseler, K. O., & Boyd, P. W. (2009). Shedding light on processes that control  
618 particle export and flux attenuation in the twilight zone of the open ocean.  
619 *Limnology and Oceanography*, *54*(4), 1210–1232.
- 620 Carozza, D. A., Bianchi, D., & Galbraith, E. D. (2016). The ecological module  
621 of BOATS-1.0: a bioenergetically constrained model of marine upper trophic  
622 levels suitable for studies of fisheries and ocean biogeochemistry. *Geoscientific*  
623 *Model Development*, *9*(4), 1545–1565.
- 624 Carozza, D. A., Bianchi, D., & Galbraith, E. D. (2017, 01). Formulation, general  
625 features and global calibration of a bioenergetically-constrained fishery model.  
626 *PLOS One*, *12*(1), 1–28. doi: 10.1371/journal.pone.0169763
- 627 Carr, M.-E., Friedrichs, M. A., Schmeltz, M., Aita, M. N., Antoine, D., Arrigo,  
628 K. R., ... others (2006). A comparison of global estimates of marine primary  
629 production from ocean color. *Deep Sea Research Part II: Topical Studies in*  
630 *Oceanography*, *53*(5), 741–770.
- 631 Cullis-Suzuki, S., & Pauly, D. (2010). Failing the high seas: A global evaluation  
632 of regional fisheries management organizations. *Marine Policy*, *34*(5), 1036 -  
633 1042. doi: <https://doi.org/10.1016/j.marpol.2010.03.002>
- 634 Dunne, J. P., Armstrong, R. A., Gnanadesikan, A., & Sarmiento, J. L. (2005).  
635 Empirical and mechanistic models for the particle export ratio. *Global Biogeo-*  
636 *chemical Cycles*, *19*(4).
- 637 Eddy, T. D., Bernhardt, J. R., Blanchard, J. L., Cheung, W. W., Colléter, M.,  
638 Du Pontavice, H., ... others (2020). Energy flow through marine ecosystems:  
639 Confronting transfer efficiency. *Trends in Ecology & Evolution*.
- 640 Eigaard, O. R., Marchal, P., Gislason, H., & Rijnsdorp, A. D. (2014). Technological  
641 development and fisheries management. *Reviews in Fisheries Science & Aqua-*  
642 *culture*, *22*(2), 156–174.
- 643 Galbraith, E. D., Carozza, D. A., & Bianchi, D. (2017). A coupled human-earth  
644 model perspective on long-term trends in the global marine fishery. *Nature*  
645 *Communications*, *8*, 14884.
- 646 Galbraith, E. D., Le Mézo, P., Solanes Hernandez, G., Bianchi, D., & Kroodsma, D.

- 647 (2019). Growth limitation of marine fish by low iron availability in the open  
648 ocean. *Frontiers in Marine Science*, 509.
- 649 Gjerde, K., Reeve, L., Harden-Davies, H., Ardron, J., Dolan, R., Durussel, C., ...  
650 others (2016). Protecting earth's last conservation frontier: scientific, manage-  
651 ment and legal priorities for mpas beyond national boundaries.
- 652 Golden, C. D., Koehn, J. Z., Shepon, A., Passarelli, S., Free, C. M., Viana, D. F., ...  
653 others (2021). Aquatic foods to nourish nations. *Nature*, 598(7880), 315–320.
- 654 Guiet, J., Aumont, O., Poggiale, J.-C., & Maury, O. (2016). Effects of lower trophic  
655 level biomass and water temperature on fish communities: A modelling study.  
656 *Progress in Oceanography*, 146, 22 - 37. doi: [http://dx.doi.org/10.1016/  
657 j.pocean.2016.04.003](http://dx.doi.org/10.1016/j.pocean.2016.04.003)
- 658 Guiet, J., Bianchi, D., Scherrer, K. J., Heneghan, R. F., & Galbraith, E. D. (2024).  
659 Boatsv2: New ecological and economic features improve simulations of high  
660 seas catch and effort. *Submitted in Geoscientific Model Development*.
- 661 Guiet, J., Galbraith, E. D., Bianchi, D., & Cheung, W. W. (2020). Bioenergetic in-  
662 fluence on the historical development and decline of industrial fisheries. *ICES  
663 Journal of Marine Science*, 77(5), 1854–1863.
- 664 Haedrich, R. L., & Merrett, N. R. (1992). Production/biomass ratios, size frequen-  
665 cies and biomass spectra in deep-sea demersal fishes. In *Deep-sea food chains  
666 and the global carbon cycle* (pp. 157–182). Springer.
- 667 Hatton, I. A., Heneghan, R. F., Bar-On, Y. M., & Galbraith, E. D. (2021). The  
668 global ocean size spectrum from bacteria to whales. *Science Advances*, 7(46),  
669 eabh3732. doi: 10.1126/sciadv.abh3732
- 670 Heilpern, S. A., DeFries, R., Fiorella, K., Flecker, A., Sethi, S. A., Uriarte, M., &  
671 Naeem, S. (2021). Declining diversity of wild-caught species puts dietary  
672 nutrient supplies at risk. *Science Advances*, 7(22), eabf9967.
- 673 Helm, R. R. (2022). Turning the tide on high-seas plastic pollution. *One Earth*,  
674 5(10), 1089–1092.
- 675 Heneghan, R. F., Galbraith, E., Blanchard, J. L., Harrison, C., Barrier, N., Bulman,  
676 C., ... others (2021). Disentangling diverse responses to climate change among  
677 global marine ecosystem models. *Progress in Oceanography*, 198, 102659.
- 678 Irigoien, X., Klevjer, T. A., Røstad, A., Martinez, U., Boyra, G., & et al., A. J. L.  
679 (2014). Large mesopelagic fishes biomass and trophic efficiency in the open  
680 ocean. *Nature Communications*, 5.
- 681 Juan-Jordá, M. J., Murua, H., Arrizabalaga, H., Merino, G., Pacoureau, N., &  
682 Dulvy, N. K. (2022). Seventy years of tunas, billfishes, and sharks as sentinels  
683 of global ocean health. *Science*, 378(6620), eabj0211.
- 684 Kerry, C. R., Exeter, O. M., & Witt, M. J. (2022). Monitoring global fishing activ-  
685 ity in proximity to seamounts using automatic identification systems. *Fish and  
686 Fisheries*, 23(3), 733–749.
- 687 Kvile, K. Ø., Taranto, G. H., Pitcher, T. J., & Morato, T. (2014). A global as-  
688 sessment of seamount ecosystems knowledge using an ecosystem evaluation  
689 framework. *Biological Conservation*, 173, 108–120.
- 690 Lam, V. W. Y., Sumaila, U. R., Dyck, A., Pauly, D., & Watson, R. (2011). Con-

- 691       struction and first applications of a global cost of fishing database. *ICES Jour-*  
692       *nal of Marine Science*, 68(9), 1996-2004. doi: 10.1093/icesjms/fsr121
- 693 Le Mézo, P. K., & Galbraith, E. D. (2021). The fecal iron pump: global impact of  
694 animals on the iron stoichiometry of marine sinking particles. *Limnology and*  
695       *Oceanography*, 66(1), 201–213.
- 696 Locarnini, R. A., Mishonov, A. V., Antonov, J. I., Boyer, T. P., & Garcia, H. E.  
697 (2006). World ocean atlas 2005, volume 1: Temperature. s. levitus. *Ed. NOAA*  
698       *Atlas NESDIS 61, U.S. Government Printing Office, Washington, D.C., 182*  
699       *pp.*
- 700 Lotze, H. K., Tittensor, D. P., Bryndum-Buchholz, A., Eddy, T. D., Cheung,  
701       W. W. L., Galbraith, E. D., . . . Worm, B. (2019). Global ensemble pro-  
702       jections reveal trophic amplification of ocean biomass declines with cli-  
703       mate change. *Proceedings of the National Academy of Sciences*. doi:  
704       10.1073/pnas.1900194116
- 705 Marra, J., Trees, C. C., & O'Reilly, J. E. (2007). Phytoplankton pigment absorption:  
706       a strong predictor of primary productivity in the surface ocean. *Deep Sea Re-*  
707       *search Part I: Oceanographic Research Papers*, 54(2), 155–163.
- 708 Martin, J. H., Knauer, G. A., Karl, D. M., & Broenkow, W. W. (1987). Vertex: car-  
709       bon cycling in the northeast pacific. *Deep Sea Research Part A. Oceanographic*  
710       *Research Papers*, 34(2), 267–285.
- 711 Maury, O. (2010). An overview of apecosm, a spatialized mass balanced “apex  
712       predators ecosystem model” to study physiologically structured tuna pop-  
713       ulation dynamics in their ecosystem. *Progress in Oceanography*, 84(1-2),  
714       113–117.
- 715 Moore, C., Mills, M., Arrigo, K., Berman-Frank, I., Bopp, L., Boyd, P., . . . oth-  
716       ers (2013). Processes and patterns of oceanic nutrient limitation. *Nature*  
717       *geoscience*, 6(9), 701–710.
- 718 Nuno, A., Guiet, J., Baranek, B., & Bianchi, D. (2022). Patterns and drivers of the  
719       diving behavior of large pelagic predators. *bioRxiv*. doi: [https://doi.org/10](https://doi.org/10.1101/2022.12.27.521953)  
720       .1101/2022.12.27.521953
- 721 Pacoureau, N., Rigby, C. L., Kyne, P. M., Sherley, R. B., Winker, H., Carlson, J. K.,  
722       . . . others (2021). Half a century of global decline in oceanic sharks and rays.  
723       *Nature*, 589(7843), 567–571.
- 724 Palomares, M. L., & Pauly, D. (2019). On the creeping increase of vessels’ fishing  
725       power. *Ecology and Society*, 24(3).
- 726 Pauly, D., Zeller, D., & Palomares, M. (2020). Sea around us concepts, design and  
727       data. Retrieved from [seararoundus.org](http://seararoundus.org)
- 728 Petrik, C. M., Stock, C. A., Andersen, K. H., van Denderen, P. D., & Watson, J. R.  
729       (2019). Bottom-up drivers of global patterns of demersal, forage, and pelagic  
730       fishes. *Progress in oceanography*, 176, 102124.
- 731 Proud, R., Cox, M. J., Le Guen, C., & Brierley, A. S. (2018). Fine-scale depth struc-  
732       ture of pelagic communities throughout the global ocean based on acoustic  
733       sound scattering layers. *Marine Ecology Progress Series*, 598, 35–48.
- 734 RAM Legacy Stock Assessment Database. (2020). *Ram legacy stock assessment*

- 735        *database v4.491*. Retrieved from <https://doi.org/10.5281/zenodo.3676088>  
736        doi: 10.5281/zenodo.3676088
- 737        Rousseau, Y., Watson, R. A., Blanchard, J. L., & Fulton, E. A. (2019). Evolution  
738        of global marine fishing fleets and the response of fished resources. *Proceedings*  
739        *of the National Academy of Sciences*, *116*(25), 12238–12243. doi: 10.1073/pnas  
740        .1820344116
- 741        Sala, E., Mayorga, J., Bradley, D., Cabral, R. B., Atwood, T. B., Auber, A., ...  
742        others (2021). Protecting the global ocean for biodiversity, food and climate.  
743        *Nature*, *592*(7854), 397–402.
- 744        Sala, E., Mayorga, J., Costello, C., Kroodsma, D., Palomares, M. L., Pauly, D., ...  
745        Zeller, D. (2018). The economics of fishing the high seas. *Science advances*,  
746        *4*(6), eaat2504.
- 747        Scherrer, K., & Galbraith, E. D. (2020). Regulation strength and technology creep  
748        play key roles in global long-term projections of wild capture fisheries. *ICES*  
749        *Journal of Marine Science*. doi: 10.1093/icesjms/fsaa109
- 750        Scherrer, K. J., Rousseau, Y., Teh, L. C., Sumaila, U. R., & Galbraith, E. D. (2023).  
751        Diminishing returns on labour in the global marine food system. *Nature Sus-*  
752        *tainability*, 1–8.
- 753        Schiller, L., Bailey, M., Jacquet, J., & Sala, E. (2018). High seas fisheries play a  
754        negligible role in addressing global food security. *Science Advances*, *4*(8),  
755        eaat8351.
- 756        Stasko, A. D., Swanson, H., Majewski, A., Atchison, S., Reist, J., & Power, M.  
757        (2016). Influences of depth and pelagic subsidies on the size-based trophic  
758        structure of beaufort sea fish communities. *Marine Ecology Progress Series*,  
759        *549*, 153–166.
- 760        Stock, C. A., John, J. G., Rykaczewski, R. R., Asch, R. G., Cheung, W. W. L.,  
761        Dunne, J. P., ... Watson, R. A. (2017). Reconciling fisheries catch and ocean  
762        productivity. *Proceedings of the National Academy of Sciences*, *114*(8), E1441-  
763        E1449. doi: 10.1073/pnas.1610238114
- 764        Sumaila, U. R., Lam, V. W., Miller, D. D., Teh, L., Watson, R. A., Zeller, D., ...  
765        others (2015). Winners and losers in a world where the high seas is closed to  
766        fishing. *Scientific Reports*, *5*(1), 1–6.
- 767        Sutton, T., Porteiro, F., Heino, M., Byrkjedal, I., Langhelle, G., Anderson, C., ...  
768        others (2008). Vertical structure, biomass and topographic association of deep-  
769        pelagic fishes in relation to a mid-ocean ridge system. *Deep Sea Research Part*  
770        *II: Topical Studies in Oceanography*, *55*(1-2), 161–184.
- 771        Tagliabue, A., Bowie, A. R., Boyd, P. W., Buck, K. N., Johnson, K. S., & Saito,  
772        M. A. (2017). The integral role of iron in ocean biogeochemistry. *Nature*,  
773        *543*(7643), 51–59.
- 774        Tittensor, D. P., Eddy, T. D., Lotze, H. K., Galbraith, E. D., Cheung, W., Barange,  
775        M., ... others (2018). A protocol for the intercomparison of marine fishery and  
776        ecosystem models: Fish-mip v1. 0. *Geoscientific Model Development*, *11*(4),  
777        1421–1442.
- 778        Tittensor, D. P., Novaglio, C., Harrison, C. S., Heneghan, R. F., Barrier, N.,

- 779            Bianchi, D., ... others (2021). Next-generation ensemble projections reveal  
780            higher climate risks for marine ecosystems. *Nature Climate Change*, 11(11),  
781            973–981.
- 782            Trueman, C., Johnston, G., O’hea, B., & MacKenzie, K. (2014). Trophic interactions  
783            of fish communities at midwater depths enhance long-term carbon storage and  
784            benthic production on continental slopes. *Proceedings of the Royal Society B:  
785            Biological Sciences*, 281(1787), 20140669.
- 786            van Denderen, P. D., Lindegren, M., MacKenzie, B. R., Watson, R. A., & Andersen,  
787            K. H. (2018). Global patterns in marine predatory fish. *Nature ecology &  
788            evolution*, 2(1), 65.
- 789            Watson, R. A. (2017). A database of global marine commercial, small-scale, illegal  
790            and unreported fisheries catch 1950–2014. *Scientific Data*, 4.
- 791            Watson, R. A., & Morato, T. (2013). Fishing down the deep: Accounting for within-  
792            species changes in depth of fishing. *Fisheries Research*, 140, 63–65.
- 793            Weber, T., Cram, J. A., Leung, S. W., DeVries, T., & Deutsch, C. (2016). Deep  
794            ocean nutrients imply large latitudinal variation in particle transfer efficiency.  
795            *Proceedings of the National Academy of Sciences*, 113(31), 8606–8611.
- 796            White, C., & Costello, C. (2014). Close the high seas to fishing? *PLoS biology*,  
797            12(3), e1001826.
- 798            Worm, B., & Branch, T. A. (2012). The future of fish. *Trends in Ecology & Evolu-  
799            tion*, 27(11), 594 - 599. doi: <https://doi.org/10.1016/j.tree.2012.07.005>

# Small fish biomass limits the catch potential in the High Seas

J. Guet<sup>1</sup>, D. Bianchi<sup>1</sup>, K.J.N. Scherrer<sup>2</sup>, R.F. Heneghan<sup>3,4</sup> and E.D.  
Galbraith<sup>5</sup>

<sup>1</sup>Department of Atmospheric and Oceanic Sciences, University of California Los Angeles, CA, United States

<sup>2</sup>Department of Biological Sciences, University of Bergen, 5020 Bergen, Norway

<sup>3</sup>Australian Rivers Institute, School of Environment and Science, Griffith University, Nathan, Australia

<sup>4</sup>School of Science, Technology and Engineering, University of the Sunshine Coast, Petrie, Australia

<sup>5</sup>Earth and Planetary Science, McGill University, Montreal, QC, Canada

## Key Points:

- Despite their vast surface area, the High Seas provide only a small fraction of global wild fish catch.
- Dispersion of trophic energy throughout deep water columns and micronutrient limitations leads to smaller fish biomass density in High Seas.
- Smaller biomass density is a major contributor to the small catch; while migration should also matter, economic factors are likely secondary.

---

Corresponding author: Jerome Guet, [jerome.c.guet@gmail.com](mailto:jerome.c.guet@gmail.com)

## Abstract

The High Seas, lying beyond the boundaries of nations' Exclusive Economic Zones, cover the majority of the ocean surface and host roughly two thirds of marine primary production. Yet, only a small fraction of global wild fish catch comes from the High Seas, despite intensifying industrial fishing efforts. The surprisingly small fish catch could reflect economic features of the High Seas - such as the difficulty and cost of fishing in remote parts of the ocean surface - or ecological features resulting in a small biomass of fish relative to primary production. We use the coupled biological-economic model BOATS to estimate contributing factors, comparing observed catches with simulations where: (i) fishing cost depends on distance from shore and seafloor depth; (ii) catchability depends on seafloor depth or vertical habitat extent; (iii) regions with micronutrient limitation have reduced biomass production; (iv) the trophic transfer of energy from primary production to demersal food webs depends on depth; and (v) High Seas biomass migrates to coastal regions. Our results suggest that the most important features are ecological: demersal fish communities receive a large proportion of primary production in shallow waters, but very little in deep waters due to respiration by small organisms throughout the water column. Other factors play a secondary role, with migrations having a potentially large but uncertain role, and economic factors having the smallest effects. Our results stress the importance of properly representing the High Seas biomass in future fisheries projections, and clarify their limited role in global food provision.

## 1 Introduction

The UN High Seas Treaty, agreed upon in March 2023, has been welcomed as an unprecedented step towards protecting the biodiversity of the global ocean (UN General Assembly, 2023). Known as the Biodiversity Beyond National Jurisdiction treaty, it explicitly calls for an integrated ecosystem approach in order to maintain and restore biodiversity and carbon cycle functioning within the 60% of the ocean area that lies beyond nationally-managed Exclusive Economic Zones (EEZs). A fundamental metric of the biodiversity that the treaty aims to protect is the abundance or biomass of marine organisms. However, because of the inaccessibility of the High Seas, and the fact that they falls outside the purview of national research organizations, the biomass of animals in the High Seas is relatively poorly evaluated.

The oceans are thought to harbour most of the remaining wild animal life on the planet (Bar-On et al., 2018). Since the High Seas cover the majority of the ocean surface, one could expect them to host a large fraction of marine life. Consistent with this expectation, roughly 67% of marine primary production is estimated to occur in the vast domain of the High Seas, even though the rate of primary production per unit area is higher in the shallow coastal waters that ring the continents (Behrenfeld & Falkowski, 1997; Carr et al., 2006; Marra et al., 2007). Given that roughly half of global primary production is marine, this implies that one third of all primary production on Earth occurs in the High Seas. Yet, the most comprehensive sampling of marine animals by humans - industrial fishing - recovers only a small fish catch from the High Seas, despite intensifying efforts (Rousseau et al., 2019). In fact, humans only retrieve about a twen-

60 tieth of the global wild fish capture – less than 0.1% of total human caloric supply – from  
61 the High Seas that cover more than half the planet (Schiller et al., 2018). We are not  
62 aware of a widely-recognized explanation for the fact that the High Seas provide so lit-  
63 tle human food.

64 On one hand, the surprisingly small High Seas catch could be explained by economic  
65 and technological constraints. Fuel and time expenditures required to travel long dis-  
66 tances, greater capital requirements for High Seas vessels, or the difficulty of catching  
67 fish in deep waters could result in higher costs of fishing the High Seas (Lam et al., 2011;  
68 Sala et al., 2018). Economic constraints can be further modulated by the variable catch-  
69 ability of the fish resource that is influenced by habitat features such as topography, or  
70 vary between gears targeting pelagic or demersal species (Palomares & Pauly, 2019; Kerry  
71 et al., 2022). On the other hand, the small fish catch relative to primary production could  
72 be a result of ecological features of the High Seas. It is possible that the High Seas have  
73 less efficient transfer of energy from primary production to fish types of commercial in-  
74 terest compared to coastal systems (Eddy et al., 2020), or that primary production in  
75 the High Seas is consumed by fish that periodically migrate to the coastal zone, lead-  
76 ing to spatial redistribution of the biomass of upper trophic levels (Block et al., 2011;  
77 Sumaila et al., 2015). To our knowledge, these alternatives have not been investigated  
78 in a consistent, integrated framework.

79 In recent years, a new generation of numerical marine ecosystem models offers a  
80 novel means to address the chronic undersampling of the High Seas. These models do  
81 not attempt to resolve individual species, but instead use fundamental empirical ecolog-  
82 ical processes to predict the growth and life history of generalized fish communities from  
83 features of the environment, including water temperature and resources from lower trophic  
84 levels, such as primary production and zooplankton biomass (Maury, 2010; Guiet et al.,  
85 2016; Blanchard et al., 2017; Tittensor et al., 2018; Heneghan et al., 2021). While these  
86 models have been designed and parameterized based on the rich observational datasets  
87 available for coastal fisheries (RAM Legacy Stock Assessment Database, 2020; Watson,  
88 2017; Pauly et al., 2020), it is possible to use their ecological principles to make predic-  
89 tions for fish production and biomass in the High Seas.

90 Figure 1 shows predictions from the Fisheries and Ecosystem Model Intercompar-  
91 ison Project (FishMIP) ensemble (Tittensor et al., 2018, 2021) for the High Seas (HS)  
92 compared to coastal seas (CS). All of them estimate a fraction of High Seas biomass,  $B$ ,  
93 relative to the global ocean surface area and primary production in the High Seas: around  
94 60% in the 1990s, the decade when global fish catches peaked (FishMIP bar in Fig. 1a,  
95 see also Appendix A to compare models). Among these models, the BOATS model sim-  
96 ulates fish catches,  $C$ , in addition to biomass by including a coupled economic module  
97 that allocates fishing effort dynamically based on the profitability of fishing at a given  
98 time in the global ocean (Carozza et al., 2016, 2017). BOATS predicts that the HS frac-  
99 tion of catch is less than that of biomass, but nonetheless far above observations at 35%  
100 of global catches in the 1990s (in blue in Fig. 1a). Furthermore, the model incorrectly  
101 simulates substantial growth in the High Seas catch and biomass fractions since 1950 (deep  
102 and light blue lines in Fig. 1b). However, both the initial High Seas catch ratio and its

103 rate of increase in BOATS greatly exceeds observations (black lines in Fig. 1a,b; catch  
104 reconstruction by Pauly et al., 2020, dashed line, and Watson, 2017, dotted line).

105 Here, we use the BOATS model and implemented new processes to test five hypothe-  
106 ses that could contribute to the discrepancies between observed and modeled High Seas  
107 catches, indirectly shedding light on the global commercial biomass distribution (see Ta-  
108 ble 1). The first two hypothesis are economic, testing the degree to which lower profitabil-  
109 ity of High Seas fishing can reasonably explain the low catches (Lam et al., 2011; Palo-  
110 mares & Pauly, 2019). The inherently higher cost involved with travelling to the deep  
111 sea, and operating gear in deep waters is explored through the hypothesis HIGHCOST.  
112 It is also conceivable that a greater dispersal of fish in the vast and deep high-seas makes  
113 it more difficult to catch the existing biomass, tested in hypothesis UNCATCHABLE.  
114 Three additional hypotheses focus on ecological reasons why there may be less biomass  
115 available in the High Seas than would be expected from primary production and water  
116 temperature alone. The limitation of phytoplankton growth because of iron limitation  
117 in high-nutrient low-chlorophyll (HNLC) regions is widely recognized (Moore et al., 2013;  
118 Tagliabue et al., 2017). While micronutrient limitation of higher trophic levels, includ-  
119 ing fish, remains unclear, multiple lines of evidence suggest that iron limitation could also  
120 retard or prevent growth of fish in the High Seas (Galbraith et al., 2019). This is cap-  
121 tured in the IRONLIM hypothesis. The ENERGOPATHS hypothesis distinguishes be-  
122 tween pelagic and benthic energy pathways, to test the possibility that deep waters pro-  
123 duce little fish biomass because the energy of primary production is dissipated in the wa-  
124 ter column before reaching benthic communities, and preferentially routed to small or-  
125 ganisms (Stock et al., 2017; van Denderen et al., 2018). Finally, the MIGRATION hy-  
126 pothesis explores the possibility that seasonal migrations deplete the High Seas of biomass  
127 by bringing “straddling” stocks into coastal waters, where they are more accessible to  
128 fishers. Straddling species represent a significant fraction of total catches (White & Costello,  
129 2014; Sumaila et al., 2015), but the fraction of biomass of these catches produced in the  
130 High Seas is unknown.

**Table 1.** List of hypotheses tested to explain the observed low High Seas vs. coastal catches and their expected effect on key variables, cost, catchability and biomass (see details Material and Methods).

Hypothesis	Cost (c)	Catchability (q)	Biomass (f)
HIGHCOST ( $S_{cost}$ )	↑ with distance/depth	-	-
UNCATCHABLE ( $S_{catch}$ )	-	↓ with depth	-
IRONLIM ( $S_{iron}$ )	-	-	↓ in HNLC regions
MIGRATION ( $S_{mig}$ )	-	-	↓ in HS, ↑ in CS
ENERGOPATHS ( $S_{ener}$ )	-	-	↓ with depth

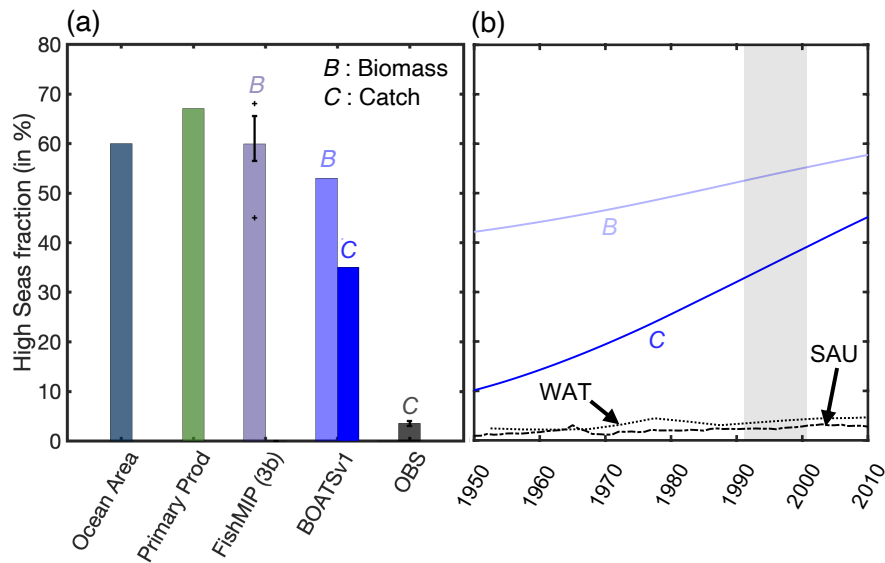


**Figure 1.** Contribution of the High Seas to the global total. (a) The High Seas fraction (%) of global ocean surface area, primary production, simulated biomass  $B$  and catch  $C$ , in the 1990s for 8 models of the FishMIP ensemble (APECOSM, DBPM, EcoOcean, EcoTroph, FEISTY, Macroecological, ZooMSS), BOATSv1, and observed catch (OBS). (b) Historical evolution of biomass,  $B$ , and catch,  $C$ , for BOATSv1 and observations. Observations are based on catch reconstructions from the Sea Around Us (SAU, dashed, Pauly et al., 2020) and Watson (2017) (WAT, dotted). The gray shading panel (b) indicates the time period used for comparisons in panel (a) and Figure 2.

## 2 Material and Methods

### 2.1 Mechanistic modeling framework

To test our hypotheses (Table 1), we use the coupled ecological-economic global marine ecosystem model BOATS to predict fish biomass and catches in the High Seas and coastal waters from environmental and economic drivers (Carozza et al., 2016, 2017). We conducted this analysis using the original BOATSV1 model and an updated version that incorporates several new features, referred to as BOATSV2 (Guet et al., 2024).

BOATS simulates the dynamics of commercial fish biomass, dependent on available resources at the base of the food web. Mean water temperature modulates the rate of biomass propagation across food webs, including production and losses. BOATS is dynamically coupled with an open-access economic module that allow simulations of fishing effort and catch dynamics. Previous work with BOATSV1 showed that the model, forced with globally homogeneous fishing costs and catchability, is able to reproduce the historical development of fisheries when driven by a uniform technological creep (3 to 8% per year, Galbraith, Carozza, & Bianchi, 2017; Guet, Galbraith, Bianchi, & Cheung, 2020). In the following sections, we discuss a series of modifications of BOATSV1 and new simulations aimed at examining our five key hypotheses.

#### 2.1.1 HIGHCOST

In BOATSV1, the cost per unit effort ( $c$ , in  $\$/W/yr$ ) is globally uniform by default. The absence of spatial dependence of cost disregards the importance of transit distance between fishing grounds and ports (Sala et al., 2018), which might be particularly relevant when comparing High Seas and coastal catches. In addition, costs are expected to rise when targeting increasingly deep fishing grounds, due to depth-dependent expenses associated with setting and hauling gears. Since demersal catches account for a large fraction of global catches, this might contribute to the delayed development of High Seas catches as deeper offshore habitats might become profitable later in time (Watson & Morato, 2013). We test both types of variable cost distributions independently under the HIGHCOST hypothesis.

For implementation, we assume that the fishing cost per unit effort is constant in coastal or shallow regions ( $c = c_{CS}$ ). Beyond these regions, the cost increases linearly, either as a function of distance to the nearest shore ( $d_{coast}$ , in  $km$ ), or as a function of seafloor depth ( $z_{bot}$ , in  $m$ ):

$$c(x = d_{coast}, z_{bot}) = \begin{cases} c_{CS} & \text{when } x \leq x^* \\ c_{CS} + \delta_c(x - x^*) & \text{when } x > x^* \end{cases} \quad (1)$$

where  $x$  represents either  $d_{coast}$  or  $z_{bot}$ ,  $x^*$  is a reference value that indirectly determines the boundary of coastal regions, and  $\delta_c$  is a parameter controlling the rate of increase of costs beyond coastal regions (in  $\$/km/W/yr$  or  $\$/m/W/yr$ , for distance to coast or bottom, respectively). We note that calculating distance to the nearest shore to mod-

167 ulate costs is a simplification, particularly for industrial fisheries. We test multiple sets  
 168 of parameters  $[x^*, \delta_c]$  (see Appendix B).

### 169 **2.1.2 UNCATCHABLE**

170 Catchability ( $q$ , in  $m^2/W/yr$ ) refers to the capturability of fish biomass per unit  
 171 effort given fish behavior (e.g. schooling, gear avoidance) and the level of technology, in-  
 172 cluding fishing gear, navigation technologies, sonar, communications and skipper knowl-  
 173 edge. Catchability generally grows exponentially over time through technological progress  
 174 (Palomares & Pauly, 2019; Eigaard et al., 2014), thus driving the historical development  
 175 of fisheries (Galbraith et al., 2017). However, the globally uniform catchability increase  
 176 in BOATSv1 does not account for geographical variations in the marine environment,  
 177 which could be significant. For example, pelagic fish in regions with vertically compressed  
 178 euphotic zones might be more accessible to purse seines than in regions where produc-  
 179 tion is spread over a larger, more diffuse vertical range (Nuno et al., 2022). Under the  
 180 UNCATCHABLE hypothesis, we incorporate spatially varying catchability to assess how  
 181 this might affect catches.

182 First, we test the scenario in which catchability varies as a function of the euphotic  
 183 layer depth ( $z_{eu}$ , in  $m$ ). Second, we test the scenario in which catchability varies as a  
 184 function of seafloor depth ( $z_{bot}$ , in  $m$ ), based on the notion that shallower regions, such  
 185 as those around seamounts or on continental shelves, promote biomass aggregation (Kvile  
 186 et al., 2014) and enhance fisheries' access to marine fish stocks (Kerry et al., 2022). The  
 187 UNCATCHABLE hypothesis tests both variable catchability distributions:

$$q(x = z_{eu}, 1/z_{eu}, z_{bot}, 1/z_{bot}, \log_{10}(z_{bot})) = q_{ref} \left[ q_{min} + (1 - q_{min}) \frac{x_{max} - x}{x_{max} - \bar{x}} \right] \quad (2)$$

188 Here  $x$  represents a function of either euphotic zone or seafloor depth,  $x_{max}$  the global  
 189 maximum of the quantity,  $\bar{x}$  the global mean, and  $q_{min}$  is a parameter that controls the  
 190 change of catchability as a function of depth. Note that we test formulations in which  
 191 catchability decreases either linearly or in proportion to the inverse of either the euphotic  
 192 zone depth or the seafloor depth (see Appendix C). In each formulation, we select  $q_{min}$   
 193 values that provide realistic spatial variations, and use  $5 \times q_{min}$  as an upper bound to catch-  
 194 ability, effectively limiting its variation to the observed range (Palomares & Pauly, 2019).  
 195 The formulation in Equation 2 modulates the global reference catchability ( $q_{ref}$ ), which  
 196 increases annually at 5% rate.

### 197 **2.1.3 IRONLIM**

198 To assess the influence of iron limitation on fish growth, we modulate the trophic  
 199 efficiency  $\alpha$ , a key parameter of BOATS that represents the fraction of organic matter  
 200 incorporated into new tissue at each trophic step:

$$\alpha = \alpha_0 \frac{k_{NO_3^-}}{k_{NO_3^-} + NO_3^-} \quad (3)$$

201 where surface nitrate concentrations ( $NO_3^-$ , in  $\mu M$ ) are taken as a proxy for low iron  
 202 conditions (Moore et al., 2013). Assuming a constant  $k_{NO_3^-} = 5 \mu M$ , this formulation  
 203 smoothly decreases the trophic efficiency relative to the reference value  $\alpha_0$  as nitrate in-  
 204 creases (Galbraith et al., 2019).

#### 205 **2.1.4 ENERGYPATH**

206 BOATSV1 calculates fish biomass from vertically integrated net primary produc-  
 207 tion ( $NPP$ ) and upper water column temperature ( $T_{75}$ ). These quantities determine fish  
 208 growth rates, and ultimately biomass accumulation, in a region. While these forcings are  
 209 relevant for pelagic species, they do not account for the flux of organic material that reaches  
 210 the seafloor as sinking particles, and sets the production of deep-sea ecosystems and fish-  
 211 eries (Blanchard et al., 2011; Stock et al., 2017; Petrik et al., 2019). Moreover, cooler tem-  
 212 peratures at the ocean bottom ( $T_{bot} < T_{75}$ ) result in slower metabolism and produc-  
 213 tion rates for deep-sea species. Both factors – organic material flux and bottom temper-  
 214 ature – must influence new fish biomass production in shallow vs. deep waters. To test  
 215 the effect of distinct drivers of production in pelagic and demersal communities, under  
 216 the ENERGYPATH hypothesis we expand BOATSV1 to provide a separate representa-  
 217 tion of pelagic species, forced by  $NPP$  and  $T_{75}$ , and demersal species, forced by the par-  
 218 ticle flux at the bottom ( $PFB$ ) and  $T_{bot}$ .

219 We derive the  $PFB$  from surface  $NPP$  (Guet et al., 2024), assuming a typical power-  
 220 law attenuation of the particle flux below the euphotic zone ( $z_{euph}$ ):

$$PFB = NPP \cdot pe_{ratio} \cdot \left(\frac{z_{bot}}{z_{euph}}\right)^{b_a} \quad (4)$$

221 where  $b_a = -0.8$  is the coefficient of attenuation of particle fluxes with depth (Martin  
 222 et al., 1987) and  $z_{euph} = 75m$  the average euphotic zone depth, which, for simplicity,  
 223 we keep constant. The term  $(z_{bot}/z_{euph})^{b_a}$  is computed first at a high resolution, using  
 224  $z_{bot}$  values from the global topographic dataset ETOPO 1/10° (Amante & Eakins, 2009),  
 225 and then averaged across each 1° grid cells of the model. Note that when  $z_{bot}$  is shal-  
 226 lower than  $z_{euph} = 75m$ , the seafloor depth is set to be equal to the euphotic zone depth.  
 227 The particle export at the base of the euphotic zone is determined by an empirical es-  
 228 timate of the particle export ratio ( $pe_{ratio}$ ), as a function of local surface temperature  
 229  $T_{75}$  and  $NPP$ , following prior work (Dunne et al., 2005).

#### 230 **2.1.5 MIGRATION**

231 At the coarse resolution of the BOATS model (1°), the horizontal transport of biomass  
 232 by currents and active movement can be assumed to play a secondary role relative to lo-  
 233 cal biomass production for many fish. However, global catches include a significant frac-  
 234 tion of straddling species that can travel large distances (Sumaila et al., 2015). While  
 235 straddling stocks are caught almost exclusively in coastal waters, some fraction of this  
 236 biomass is produced from trophic energy foraged in the High Seas. Fish migration and  
 237 subsequent capture in coastal seas therefore represents a flux of trophic energy from the  
 238 high seas to coastal waters that is not resolved by BOATS. This biomass flux could con-

239 tribute to the discrepancy between modelled and observed catches in the High Seas vs.  
240 coastal regions.

241 Unfortunately, the considerable uncertainty in behavioural drivers of fish migra-  
242 tion prevents an explicit representation of this biomass redistribution at this time. Thus,  
243 unlike the mechanisms described above, we do not include migration as a mechanistic  
244 component of the model. Instead, we gauge the effect of fish migrations by estimating  
245 a plausible contribution of High Sea biomass to the total catch in each EEZ  $i$ , based on  
246 the simulated catch ( $C_i$ ) inside the EEZ, and the fraction of total catch in the EEZ that  
247 can be attributed to straddling species ( $\alpha_{str,i}$ ), which we estimate based on observational  
248 catch reconstructions (see Appendix D):

$$C_i = C_i^{adj} - \delta_s \alpha_{str,i} C_i^{adj} \quad (5)$$

249 where  $C_i^{adj}$  is the total catch adjusted for straddling species in a given EEZ, and the ar-  
250 bitrary factor  $\delta_s$  represents the proportion of the catch of straddling species coming from  
251 the High Seas. This factor provides an indirect measure of the coastal catch contribu-  
252 tion by fish biomass produced in the High Seas. Rearranging terms in Equation 5 pro-  
253 vides an estimate of the total catch  $C_i^{adj}$  from simulated catch within each EEZ  $C_i$ :

$$C_{CS}^{adj} = \sum_{EEZ_s} C_i^{adj} \quad (6)$$

$$C_{HS}^{adj} = C_{HS} - \sum_{EEZ_s} (C_i^{adj} - C_i). \quad (7)$$

254 Ultimately, we use  $C_{CS}^{adj}$  and  $C_{HS}^{adj}$  as updated coastal and High Seas catches after biomass  
255 redistribution by migration of straddling species, as long as  $C_{HS}^{adj} > 0$ . Given that  $\delta_s$   
256 is undetermined, we use a range of values to estimate the magnitude of biomass trans-  
257 fer, and add the resulting High Seas-derived straddling catch to the Coastal Catch.

## 258 2.2 Simulations

259 Our five hypotheses (Table 1) are tested with new simulations compared to the ref-  
260 erence simulation made with BOATSV1 (shown in blue in Fig. 1, hereafter simulation  
261  $S_{v1}$ ). In order to capture uncertainty in model parameters, we run each experiment with  
262 a small ensemble of 5 different parameter sets (Carozza et al., 2017). We take the en-  
263 semble mean as the final result, and when relevant use the spread across the 5 members  
264 as a measure of uncertainty.

265 We first compare means and uncertainties for new simulations that update the ref-  
266 erence model to include economic constraints ( $S_{cost}$  and  $S_{catch}$ , Table 1). Second, we com-  
267 pare new simulations that test the influence of ecological features ( $S_{iron}$  and  $S_{ener}$ ). Be-  
268 cause simulation  $S_{ener}$  changes the structure of the ecological model, we generated 5 new  
269 parameter sets by running a new optimization with a Monte-Carlo ensemble using the  
270 BOATSV2 code (Guet et al., 2024). Similar to the BOATSV1 parameter ensemble, the  
271 BOATSV2 parameter sets were selected to best capture global observations including the  
272 catch peak aggregated by Large Marine Ecosystems (LMEs), and the spatial variabil-

ity of historical catch maxima in each LME. BOATSv1 and v2 are both tuned based on similar coastal observations, resulting in comparable dynamics in coastal seas. However, they markedly differ in their representation of the High Seas. Finally, we evaluate the role of straddling species by adjusting catch *a posteriori* from the reference simulation ( $S_{mig}$ ).

Simulations are run on a  $1^\circ$  global grid, forced with climatological observations of the surface mean temperature between 0 and 75m ( $T_{75}$ ) and the temperature near the seafloor ( $T_{bot}$ ) from the World Ocean Atlas (Locarnini et al., 2006). We estimated  $T_{bot}$  as the mean temperature in the water column weighted by the fraction of each depth in a model grid cell as reported by ETOPO  $1/10^\circ$  (Amante & Eakins, 2009). For net primary production, we take the average of three satellite-based estimates to capture some of the variability inherent to primary production models (Behrenfeld & Falkowski, 1997; Carr et al., 2006; Marra et al., 2007). To parameterize iron limitation in HNLC regions we take the monthly minimum surface nitrate in the World Ocean Atlas climatology (Locarnini et al., 2006).

### 2.3 Observational constraints

To evaluate our hypotheses against observations, we use two spatially explicit reconstructions of global catches: SAU, the Sea Around Us from Pauly et al. (2020); WAT, from Watson (2017). Both provide global catches at  $1^\circ$  resolution from 1950 to 2014, and are corrected for unreported catches. We focus on the following two indicators:

- (i) The fraction of catch occurring in the High Seas relative to the total catch. We compare this ratio around the global catch peak of the 1990s ( $\pm 5$  years around 1996, gray shading in Fig. 1), for which observations suggest a mean value of 3-4% (*OBS* in Fig. 1a). For each simulation, we average the 11 years of catch around the peak of catch summed across EEZ, and report the mean and spread (10th to 90th percentiles) of the 5 ensemble members.
- (ii) The historical deepening of the global catch. The deepening of catches over time serves as an indicator of the rate at which fisheries develop in deep vs. shallow regions. The mean observed seafloor depth weighted by the local catch in the 1990s is 372m in SAU and 154m in WAT. We compare these estimates with the mean depth for the 11-year period around the catch peak across EEZs in the model simulations, reporting the ensemble mean and spread.

Once the relevant hypotheses are identified, we further evaluate their contribution to global fisheries' development by independently comparing simulated catches with pelagic and demersal catch reconstructions from the SAU (see Appendix E for the definition of demersal and pelagic groups). We also compare regional catch variations across LMEs and 11 High Seas ecosystems when sequentially including new processes (HSEs, Appendix F).

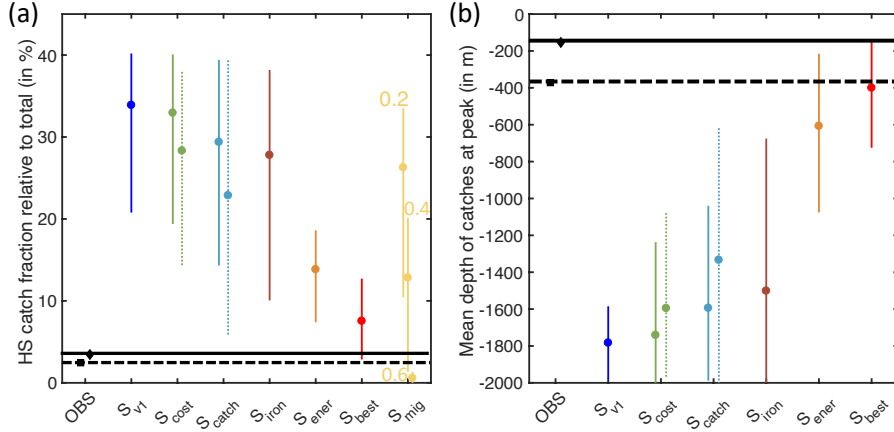


**Figure 2.** Influence of the hypothesized mechanisms (Table 1) on High Seas fisheries development. (a) Observed and simulated High Seas catch fraction. (b) Observed and simulated mean depth of catches. Values reflect the global catch peak of the 1990s. Simulations are compared with reconstructions from the SAU (black squares and dashed horizontal lines, Pauly et al., 2020) and WAT databases (black diamonds and solid horizontal lines, Watson, 2017). Both panels show the model’s ensemble mean and 10-90th percentile range, for each simulation set. In both panels, solid and dotted ranges indicate model variants with distinct parameterizations, i.e., distance- or depth-dependent costs for  $S_{cost}$ , euphotic layer- or seafloor- dependent catchability for  $S_{catch}$ . In panel (a), for  $S_{mig}$ , each range corresponds to a distinct value of the factor  $\delta_s$ , as reported on the figure.

### 3 Results and discussion

#### 3.1 Small effect of economic constraints

Both hypotheses related to economic mechanisms (HIGHCOST and UNCATCHABLE) are unable to correct the excessive High Seas catches of the reference simulation  $S_{v1}$  when keeping realistic parameterizations (see  $S_{cost}$  in green and  $S_{catch}$  in light blue, Fig. 2a). Higher fishing costs in the High Seas within the range of observations (i.e., [6.94-8.87]\$/W/yr, Sala et al. (2018)) only decrease the fraction of High Seas catches to, on average, 29% (from 35%), while delayed development of fisheries in offshore regions for spatially variable catchability (with deeper euphotic zones and bottom depths) decreases the fraction to 23%. Both remain high compared to the observed 3-4% (see Appendices B,C).

The shift of global catches to shallower fishing grounds is also insufficient for both economic hypotheses (Fig. 2b). But, improvements are substantial, especially when applying depth-dependent fishing costs and catchabilities (Appendices B,C). Access to deep demersal stocks or aggregation of pelagic biomass around seamounts and in shallow regions can contribute to the slow deepening of fishing through time.

### 3.2 Large effect of energy pathways

Among hypotheses related to ecological mechanisms (IRONLIM and ENERGY-PATH), iron limitation of fish partially reduces the mean High Seas catch ratio (down to 28% on average, see  $S_{iron}$ , brown line in Fig. 2a). The magnitude is comparable to other economic hypotheses. While allowing the pelagic and demersal communities to develop independently from separate food resources at low trophic levels significantly corrects the fraction (down to 13%, see  $S_{ener}$ , orange line in Fig. 2a). These improvements are consistent with a reduced High Seas catch fraction attributable to lower fish biomass production in the High Seas compared to coastal waters.

Similar to other economic constraints, with iron limitation the mean depth of catch remains much deeper than observed (brown line in Fig. 2b). Iron limitation might influence biomass production and thus fisheries yields in the High Seas, yet a link with seafloor depth is lacking. In contrast, having independent pelagic and demersal communities allows a more abundant demersal biomass in shallow waters, which support larger coastal fisheries and ultimately reduces the historical deepening of global catches (orange line in Fig. 2b). Our simulations of the ENERGYPATH hypothesis indicate that it is a fundamental mechanism leading to relatively low catches in the High Seas.

### 3.3 Combined economic and ecological effects

Taken in isolation, ecological features limiting biomass production in High Seas best explain the smaller High Sea catches (IRONLIM and ENERGYPATH), while economic constraints are insufficient (HIGHCOST and UNCATCHABLE). However, the inclusion of economic constraints could still influence spatio-temporal dynamics.

Historically, observed demersal catches are largely coastal (60 times larger inside EEZ than High Seas in 2000s, compare black solid and dotted lines in Fig. 3a), while pelagic catches are more evenly distributed between coastal waters and the High Seas (20 to 1 in 2000s, Fig. 3b). When the ecological features are implemented in BOATS, they largely capture the historical variation of catch for each functional type, with slight overestimation of High Seas catches (orange lines in Fig. 3). Yet, development of High Seas fisheries still occurs in the model and becomes increasingly over-estimated after 1990. The selected economic constraints mitigate this bias by reducing catch on the more homogeneously distributed pelagic biomass (red lines in Fig. 3). For instance, with depth-dependent demersal fishing costs and depth-dependent pelagic catchabilities, the fraction of High Seas catch reaches 8% for a mean depth of catch of 400m, close to observation (see  $S_{best}$  Fig. 2).

Spatially (Fig. 4), the addition of ecological features corrects the simulated catch densities across LMEs and HSEs (from  $R=0.73$  to  $0.83$ , while RMSE is halved, Figs. 4a,b). The correction is especially important in regions over deeper seafloors (compare color shadings in Figs. 4a,b). In shallower coastal regions, yields remain comparable, as pelagic and demersal communities experience similar environmental forcing (compare circles in Figs. 4a,b). In deeper regions, especially in the High Seas, yields drop markedly, in agreement with a lower biomass production (compare darker markers and triangles). Economic

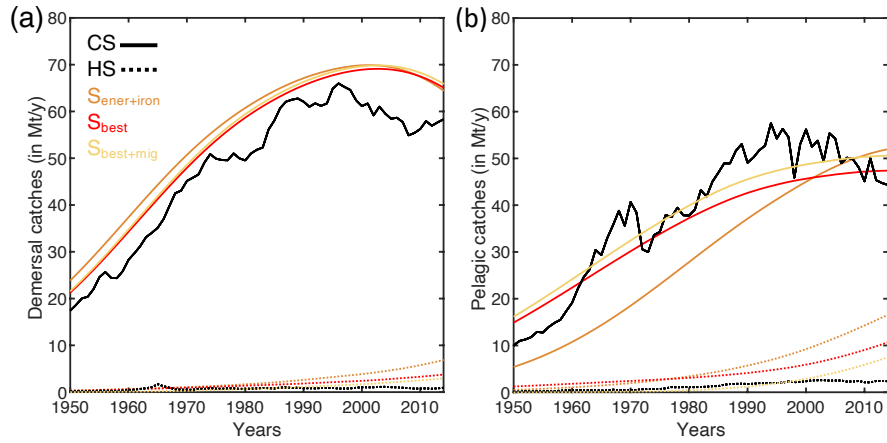


**Figure 3.** Historical evolution of pelagic and demersal catch. (a) Historical demersal fish catch. (b) Historical pelagic fish catch. In each panel, the solid lines indicate catches inside EEZs, while dotted lines indicate catches in the High Seas. Simulations including ecological corrections ( $S_{ener+iron}$  in orange), ecological and economic corrections ( $S_{best}$  in red), and correction for straddling biomass ( $S_{best+mig}$  in yellow).

368 features have a smaller effect (correlation from  $R=0.83$  to  $0.84$ , RMSE decreases from  
 369  $0.16$  to  $0.11$ , Figs. 4b,c). The influence of depth on costs and catchability further delays  
 370 the development of fisheries in High Seas, ultimately reducing yields at the peak in the  
 371 1990s (compare triangles in Figs. 4b,c). Economic constraints must have impacted the  
 372 development of High Seas fisheries, yet their effect on the small High Seas catch fraction  
 373 is secondary compared to the mechanisms that govern the global fish biomass distribu-  
 374 tion.

375 Together, the selected economic and ecological hypotheses explain the variability  
 376 of global catch with high fidelity (compare spatial distributions in the 1990s, Figs. 4d  
 377 and e). Notable mismatches remain in the Western Equatorial Pacific, which supports  
 378 larger fisheries than simulated by the model, and in Arctic waters, where the model over-  
 379 estimates catches. Our definition of economic constraints could influence the mismatches,  
 380 or these indicate missing processes. New observational metrics will be necessary to weigh  
 381 the effect of these mechanisms. While fisheries management must also influence regional  
 382 dynamics (K. Scherrer & Galbraith, 2020), smaller High Seas catches primarily results  
 383 from lower biomass densities in these regions.

### 384 3.4 Migration redistributes biomass

385 Thus far, we have not addressed the role of migrating fish biomass from High Seas  
 386 to the coast. Our analysis shows that straddling species, migrating between coastal wa-  
 387 ters and the High Seas, are caught in many high latitude and subtropical insular EEZs,  
 388 where they often contribute more than 80% of local catches (see Appendix D). This could  
 389 represent a large biomass transfer from the High Seas to the coast, if the fish are ener-  
 390 getically supported by High Seas primary production through a significant part of their

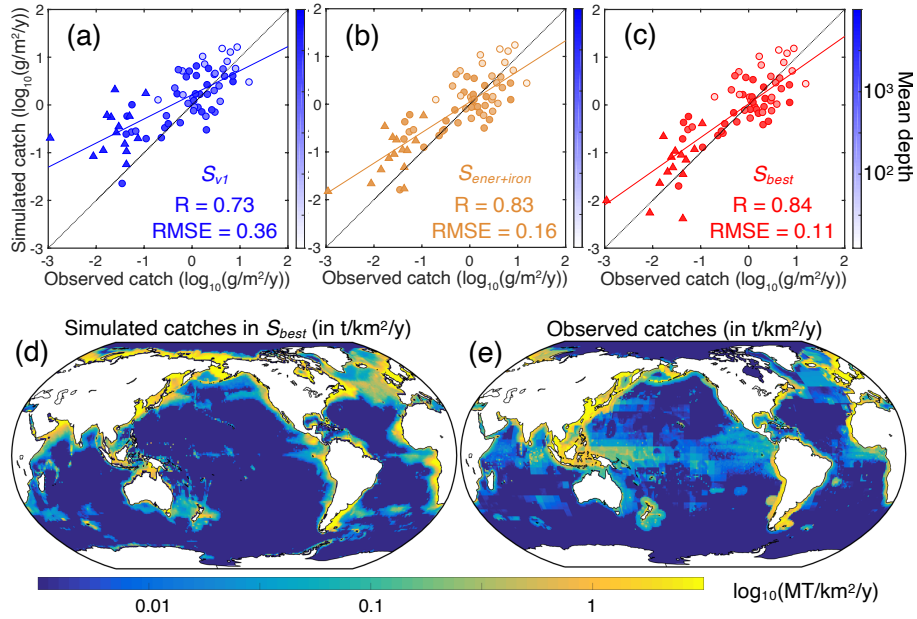


**Figure 4.** Regional catch variation at the global peak in the 1990s. Observed vs. simulated mean catch densities by regions of the global ocean for: (a) the reference simulations  $S_{v1}$ ; (b) simulations including ecological features that limit production in the High Seas (HS)  $S_{ener+iron}$ ; (c) simulations including ecological features and economic constraints  $S_{best}$ . (d) Map of simulated global catches at peak for the best simulations including ecological and economic features influencing catch in the HS, at global peak. (e) Map of observed global catches at peak. Panel (a-c), the circular markers indicates LMEs, the triangles HSEs (see Appendix F), the lines show linear fits across data, and the shadings indicate variations in the mean depth of each region, on a log10 scale (in  $m$ ).

391 life cycle. Assuming that, for example, 50% of straddling catch is derived from High Sea  
 392 production (i.e., 40% of total catch, where 80% of the catch is straddling) would bring  
 393 the modelled High Seas to coastal seas catch ratio closer to observations (see  $S_{mig}$  Fig. 2a,  
 394 yellow line). However, to maintain realistic High Seas catches (i.e., about 4  $Mt/y$ ), the  
 395 adjustment of the reference simulation ( $S_{v1}$ ) would require a migration of more than 60%,  
 396 which would imply a catch fraction much smaller than observed ( $1 < \%$ , Fig. 2a). Thus,  
 397 migration could be a very important contributor, but is insufficient alone to explain the  
 398 small catches in the High Seas.

399 This analysis highlights the potential for migration of straddling species to natu-  
 400 rally extract biomass from the High Seas, since, as long as High Seas biomass density  
 401 remains lower than coastal seas, migrating biomass will be caught more profitably in coastal  
 402 regions. When High Seas catches are reduced by lower High Seas biomass (best simu-  
 403 lation,  $S_{best}$ ), correction or remaining discrepancies between the model and observations  
 404 would require setting 5% of demersal and 10% of pelagic coastal catches on straddling  
 405 species to come from the High Seas (compare red and yellow lines in Fig. 3). These val-  
 406 ues modulate the excessive development of High Seas fishing, while allowing realistic High  
 407 Seas catches (4  $Mt/y$ ) and are, therefore, plausible. But migration is hard to constrain,  
 408 and more work is required to link regions of biomass production to biomass extraction  
 409 that goes beyond the scope of this study.

### 410 3.5 Small High Seas fish biomass and implications

411 The small High Seas catch fraction requires that, for the same level of primary pro-  
 412 duction, High Seas produce less biomass of commercially targeted fish (see  $S_{best}$  Fig. 2).  
 413 Based on our results, the dominant mechanism behind this small production is the sep-  
 414 aration of prey resources for pelagic and demersal communities (ENERGYPATH).

415 Both prey resources,  $NPP$  and  $PFB$ , are available at distinct relative abundances  
 416 in High Seas and coastal seas (see  $PFB/NPP$  ratios in Fig. 5a). In coastal seas, dem-  
 417 ersal resources from particle fluxes are on average  $10\times$  less abundant than  $NPP$ . This  
 418 proportion decreases to  $100\times$  less abundant in the High Seas, because of the increased  
 419 dissipation of energy of primary production over deeper water columns. Within each re-  
 420 gion, other mechanisms must compensate for less abundant demersal resources to allow  
 421 comparable pelagic and demersal biomass densities (Fig. 5b), ultimately explaining the  
 422 similar magnitude of demersal and pelagic catches in observations (Fig. 3).

423 A likely candidate mechanism is that, in demersal communities, the processing of  
 424 detritus by large detritivores in benthic ecosystems shortens the length of food chains  
 425 before energy reaches the exploitable demersal fish biomass. In BOATS, food chains are,  
 426 on average, shorter by 1 to 1.4 trophic levels in coastal and High Seas respectively (Fig. 5c).  
 427 For an average trophic efficiency of 0.1, such compensation can correct the factor-of-10  
 428 discrepancy in coastal seas, but is insufficient to correct the factor-of-100 discrepancy  
 429 in High Seas. In summary, shorter demersal food chains support larger demersal biomass  
 430 than pelagic biomass in coastal areas. In the High Seas, a larger proportion of the en-

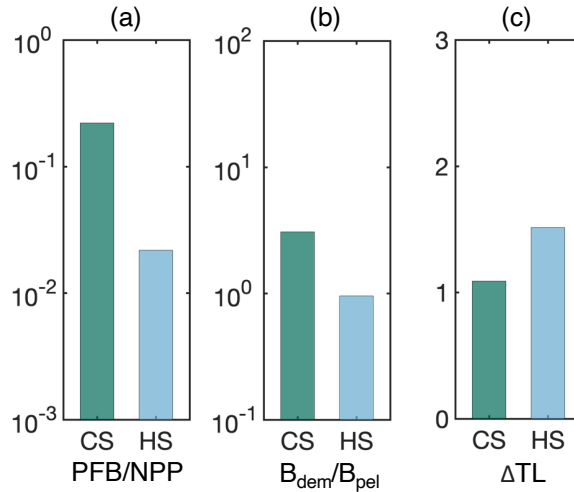


**Figure 5.** Drivers of the difference in pelagic and demersal biomass. (a) Ratio of low trophic level resources ( $PFB/NPP$ ) for demersal vs. pelagic communities. (b) Demersal vs. pelagic biomass ratio ( $B_{dem}/B_{pel}$ ). (c) Trophic distance of fish recruits relative to the representative size of the low trophic level prey. Each unit indicates one additional trophic level for the pelagic community relative to the demersal community. Green and blue bars show coastal (CS) and High Seas (HS) respectively. The ratios are means for the global ocean, weighted by fish biomass and with masked HNLC regions.

431 energy available from photosynthesis is lost, leading to a smaller biomass density per unit  
 432 of  $NPP$ .

433 Our best simulation shows a notable contrast in the change of biomass over time  
 434 between High Seas and coastal waters. In the early 20th century, the total biomass of  
 435 commercially-targeted fish in coastal waters is 1.8 Gt, 2-3 times larger than that of the  
 436 High Seas. The subsequent extraction of commercial fish in coastal regions causes coastal  
 437 biomass to decline to only 0.8 Gt by 2013 (Fig. 6), a rate of decline comparable to a pre-  
 438 vious analysis (Worm & Branch, 2012; Bianchi et al., 2021). As a result, the model sug-  
 439 gests that the High Seas presently harbor a similar amount of biomass as coastal regions,  
 440 but spread over a much larger area, and that the fraction of global fish biomass in the  
 441 High Seas has increased from 30% to 50%. We note that our simulations do not include  
 442 migrations, which would have caused the High Seas biomass to decrease by a larger amount.  
 443 Without effective fisheries management (i.e., under open-access dynamics), economic the-  
 444 ory suggests that fishing will eventually even out the biomass distribution across High  
 445 Seas and coastal regions, and continual increases in price and/or technological progress  
 446 will render previously unprofitable regions suitable for exploitation (compare High Seas  
 447 and coastal seas biomass in Fig. 6).

## 448 4 Conclusion

449 We shed light on why so few fish are caught in the High Seas by testing a suite of  
 450 hypotheses using a global fisheries model constrained by global catch observations. Our

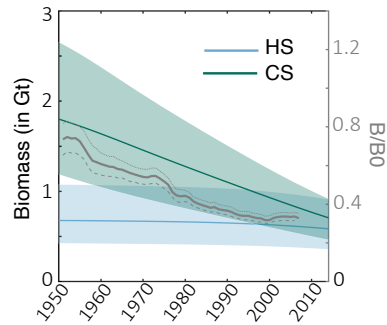


**Figure 6.** Historical evolution of global biomass under fishing. The green and blue colors show coastal and High Seas respectively, the envelopes the 10-90th percentile ranges for each simulation set, and the gray lines the observed change in biomass based on stock assessments (Worm & Branch, 2012).

451 results indicate that the primary factor is simply that the biomass of commercially tar-  
 452 geted fish in the High Seas is small compared to that of coastal waters. This is an im-  
 453 portant insight for global marine ecosystem modeling efforts (Lotze et al., 2019; Titten-  
 454 sor et al., 2021) as many models predict large High Seas biomass fraction (see the mean  
 455 of FishMIP ensemble in Fig. 1a). Our simulations provide ecologically feasible mecha-  
 456 nisms to explain this discrepancy, including the dependence of trophic pathways on wa-  
 457 ter depth, and micronutrient limitation. Economic constraints alone cannot explain the  
 458 low fish catches in the High Seas, but likely modulate the rate of development of High  
 459 Seas fisheries. Finally, migration of straddling species from the High Seas to coastal re-  
 460 gions is difficult to represent and quantify, but is likely to play a significant role in de-  
 461 pleting High Seas fish populations by exposing them to fishing effort in coastal waters.  
 462 In essence, a significant fraction of High Seas fish may be caught when they migrate to  
 463 coastal waters, without the need to fish far from port.

464 We suggest that the most important ecological factor explaining the low High Seas  
 465 catches is the impact of water depth on organic matter consumption (Buesseler & Boyd,  
 466 2009). In coastal seas, the concentration of organic production in a thin layer, with fewer  
 467 trophic steps between primary producers and commercial fish, allows a much larger por-  
 468 tion of the energy to be channeled to the large organisms humans prefer to eat, and sup-  
 469 ports demersal species that dominate on upper shelf slopes (Haedrich & Merrett, 1992;  
 470 Stasko et al., 2016). In the High Seas, the outputs of primary production are volumet-  
 471 rically diluted, and are consequently consumed by microbes and filter feeders over an ex-  
 472 tended vertical range of the water column, without accumulating in sufficiently high den-  
 473 sity to support abundant populations of large fish. Note that mechanisms that couple  
 474 pelagic and demersal communities could modulate this difference, such as vertical mi-  
 475 grations that enable predator-prey interactions across overlapping vertical habitats (Sutton  
 476 et al., 2008; Trueman et al., 2014). The lack of trace nutrients may also contribute to  
 477 the sparsity of the pelagic community, for example the low availability of the essential  
 478 element iron in waters far from shore (Galbraith et al., 2019). As a result, there are fewer

479 commercially valuable fish to be found in the High Seas. We note that small mesopelagic  
480 fish may be abundant in the High Seas, particularly where primary production is ele-  
481 vated (Irigoien et al., 2014; Proud et al., 2018). The relatively high abundances of mesopelagic  
482 fish can be attributed to their ability to intercept dispersed sinking fluxes, and a lower  
483 susceptibility to iron limitation (Le Mézo & Galbraith, 2021). We have not attempted  
484 to explicitly quantify mesopelagic fish here given that they are not commercially exploited  
485 at present and therefore cannot be constrained by catch records, a key part of our method-  
486 ology.

487 Our results support prior work emphasizing that the High Seas cannot provide a  
488 significant amount of wild fish for direct human consumption (Sumaila et al., 2015; Schiller  
489 et al., 2018). Although wild fish are relatively nutrient-rich (Golden et al., 2021; Heilpern  
490 et al., 2021), the rate at which they are produced is small compared to the overall hu-  
491 man food system, which is dominated by terrestrial agriculture (K. J. Scherrer et al., 2023),  
492 and the potential of the High Seas to provide additional food is minimal. This is also  
493 consistent with historical evidence showing that fisheries in the High Seas have decimated  
494 populations of top predators (Cullis-Suzuki & Pauly, 2010; Pacoureau et al., 2021; Juan-  
495 Jordá et al., 2022), altering the size structure of the overall community (Hatton et al.,  
496 2021), despite providing limited food to humans. Instead of food provision, closing the  
497 High Seas to fishing would have the potential benefits of increasing High Seas biodiver-  
498 sity (Gjerde et al., 2016; Sala et al., 2021), reducing fishing gear waste (Helm, 2022), and  
499 eliminating costly subsidies and fuel-inefficient fishing practices (White & Costello, 2014;  
500 Sala et al., 2018). Timely protection of High Seas ecosystems may help buttress them  
501 against increasing pressures to intensify fishing as technological innovations cause them  
502 to become financially more attractive despite their low fish biomass density.

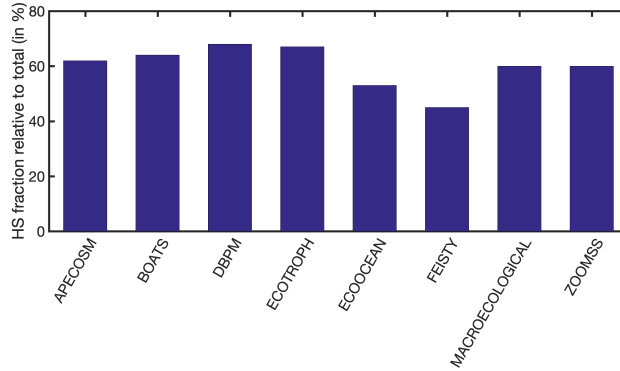


**Figure A1.** Mean contribution of the High Seas biomass to the global total per FishMIP model of the ISIMIP3b simulations forced with IPSL-CM6A-LR (Tittensor et al., 2021).

### 503 **Appendix A High seas biomass fraction in FishMIP models**

504 Despite large differences in model structure, global fish biomass models suggest a  
505 comparable fraction of High Seas to coastal seas biomass.

### 506 **Appendix B Variable fishing costs**

507 The cost of fishing varies per fishing gear, per fish community targeted (Lam et al.,  
508 2011). To best constrain spatially variable costs we use estimates of these separate fish-  
509 ing costs in the high-seas (HS) for the main gear types (98% of total effort) following data  
510 reported by Sala et al. (2018). Table B1 summarizes these estimated costs. These com-  
511 pare with BOATS's default fishing cost of 5.85\$/W/yr (Carozza et al., 2017; Galbraith  
512 et al., 2017).

513 Figure B1 summarizes the effect of spatially heterogeneous fishing costs on the ra-  
514 tio HS vs. CS catch, on the variations of the mean depths above which catch occur, as  
515 well as the global mean HS fishing cost, once weighted by effort.

516 First, increasing the cost of fishing with distance to nearest shore [ $x^* = 370, \delta_d$ ]  
517 can partly correct the ratio of catches between HS and CS (Fig. B1a). But most catch  
518 remain over deep seafloor, unlike suggested by observation (mean depth of catch  $\approx 1000$ m  
519 Fig. B1b).

520 Second, increasing the cost of fishing with seafloor depth [ $x^* = 200, \delta_z$ ] can cor-  
521 rect both the ratio of catches between HS and CS, and contributes to the shallowing of  
522 the mean seafloor depth of catches Figs. B1a,b). But, this correction corresponds to un-  
523 realistic high HS fishing costs ( $\approx 8.87$ \$/W/yr, upper range of observed costs Fig. B1c),  
524 inconsistent with observation (Tab. B1).

525 In both cases, spatially variable fishing costs within the range of observation can  
526 not account for the small fraction of HS vs. CS catches. We tested the effect of separate  
527 costs  $\delta_{d,z_{bot}}$ , adjustment of the parameter  $x^*$  only slightly modify the results. For a re-

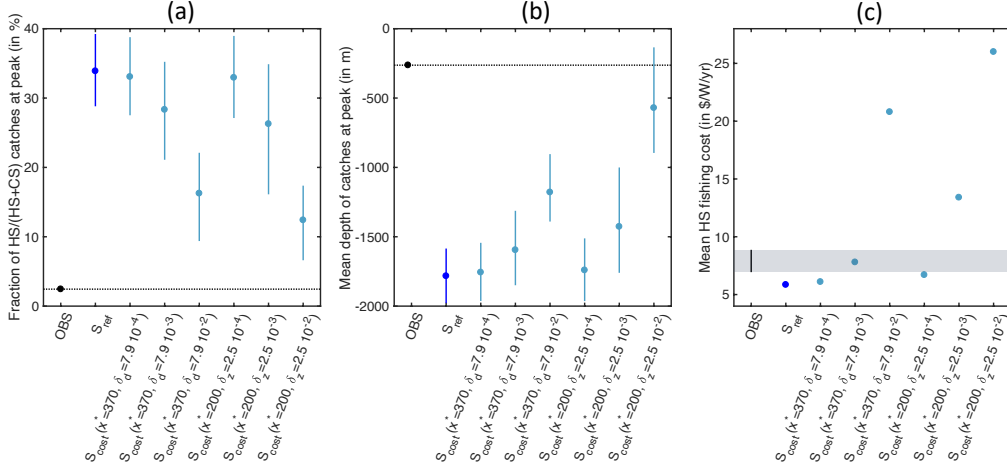


**Figure B1.** Effect of spatially heterogeneous costs. (a) Observed and simulated fraction of HS vs. CS catches at global peak for multiple model variants. (b) Observed and simulated mean depth of catches at global peak for multiple model variants. (c) Observed and simulated mean HS fishing costs once weighted by local fishing effort, around 2010. Panels (a,b) show the ensemble mean as well as the 25-75th percentile ranges per simulation set compared to observation, black dot and horizontal dotted line. Panel (c) shows mean simulated costs and how they compare to the range of observation Tab. B1 (grey shading).

528 alistic cost of fishing the high seas the correction of HS vs. CS ratio seems impossible.  
 529 We conclude that cost alone does not explain the smaller exploitation of the high-seas.

**Table B1.** Cost of fishing the high-seas based on estimates from Sala et al. (2018) for year 2016.

Gear type	Effort in kWh (fraction of total)	Cost range in \$	Cost per unit effort in \$/W/yr
Trawlers	979 10 <sup>6</sup> (15%)	[750 10 <sup>6</sup> -1030 10 <sup>6</sup> ]	[6.7-9.2]
Long liners	3719 10 <sup>6</sup> (55%)	[2523 10 <sup>6</sup> -3023 10 <sup>6</sup> ]	[6.0-7.1]
Purse seiners	394 10 <sup>6</sup> (6%)	[702 10 <sup>6</sup> -1188 10 <sup>6</sup> ]	[15.7-26.0]
Squid jiggers	1490 10 <sup>6</sup> (22%)	[1308 10 <sup>6</sup> -1616 10 <sup>6</sup> ]	[7.7-9.5]
Range all gears	(98%)	-	[6.94-8.87]
BOATS default	-	-	5.85

### Appendix C Variable biomass catchabilities

530  
 531 The catchability of fish biomass per unit effort can vary between species (e.g. school-  
 532 ing or dispersed species), depending on the preferred depth inhabited by these species,  
 533 from the surface to the limit of the euphotic layer depth and to the seafloor. To constrain  
 534 the spatially variable catchabilities, we compare with estimates of the variability of tech-  
 535 nology coefficients per fishing gears as detailed in Palomares and Pauly (2019). Table C1

536 summarizes these estimated coefficients and how they vary. In BOATS the coefficients  
 537 are spatially homogeneous (value of 1) by default.

538 Figure C1 summarizes the effect of spatially variable catchabilities on the ratio HS  
 539 vs. CS catch, and on variations of the mean depths above which catch occur.

540 The spatial variation of catchability as a function of the depth of the euphotic layer  
 541 ( $z_{eu}$ ,  $1/z_{eu}$ ,  $\log_{10}(z_{eu})$ ) or seafloor depth ( $z_{bot}$ ,  $\log_{10}(z_{bot})$ ) only allows a limited redi-  
 542 stribution of catches from the high seas to the coast (Fig. C1a). The mean depth over  
 543 which fishing occurs is also partially corrected with each profile (Fig. C1b).

544 Allowing spatially variable catchabilities while keeping the range within observa-  
 545 tional ranges (Table C1) does not allow correction of the delayed development of high  
 546 seas fisheries compared to coastal ones. We conclude that catchability alone can not ex-  
 547 plain the smaller exploitation of the high-seas. However, slight variations of the catch-  
 548 ability could contribute to explain the overall shallow depth of catch, especially when  
 549 catchability varies with  $\log_{10}(z_{bot})$  (Fig. C1b).

**Table C1.** Technology coefficients per fishing gear based on estimates from Palomares and Pauly (2019) for year 1995 (relative to mean).

Gear type	Technology coefficient
Super trawler	1.19
Freeze trawler	0.95
Stern trawler	0.90
Trawlers	0.86
Shrimp trawler	1.05
Tuna seiner	0.76
Tuna longliner	1.10
Purse seiner	0.95
Longliner	1.33
Gillnetter	0.71
Multipurpose	1.19
Range all gears	[0.71-1.33]
BOATS default	1

## 550 Appendix D Straddling fraction per EEZ

551 The migration of fish biomass can influence the spatial correlation of regions where  
 552 biomass is produced and where it is caught by fisheries. While the straddling fraction  
 553 of catch in an EEZ does not necessarily reflect the fraction of biomass produced outside  
 554 this region, it provides an estimate of the plausible range of redistribution. We inferred  
 555 the straddling catch fraction from Sea Around Us (SAU) reported catch per species within  
 556 each EEZ, separately summing catch on species solely caught inside EEZs ( $C_{EEZ}^{loc}$ ), and  
 557 catch on species caught both in EEZs and highseas ( $C_{EEZ}^{str}$ ,  $\alpha_{str} = C_{EEZ}^{str}/(C_{EEZ}^{str} +$   
 558  $C_{EEZ}^{loc})$ ). We use the list of species in Sumaila et al. (2015) for this distinction. Figure D1a

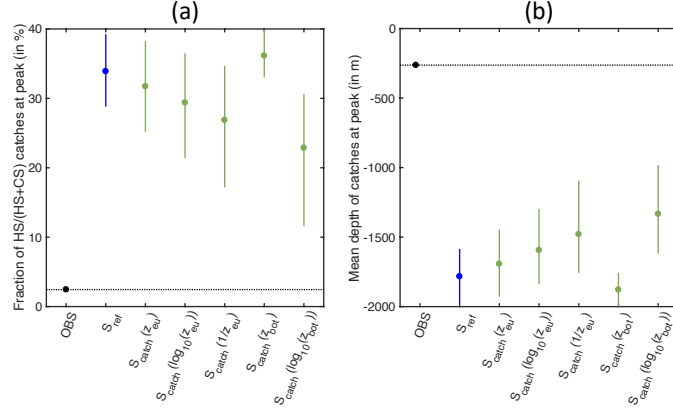


**Figure C1.** Effect of spatially heterogeneous catchabilities. (a) Observed and simulated fraction of HS vs. CS catches at global peak for multiple model variants. (b) Observed and simulated mean depth of catches at global peak for multiple model variants. Panels (a,b) show the ensemble mean as well as the 25-75th percentile ranges per simulation set compared to observation, black dot and horizontal dotted line.

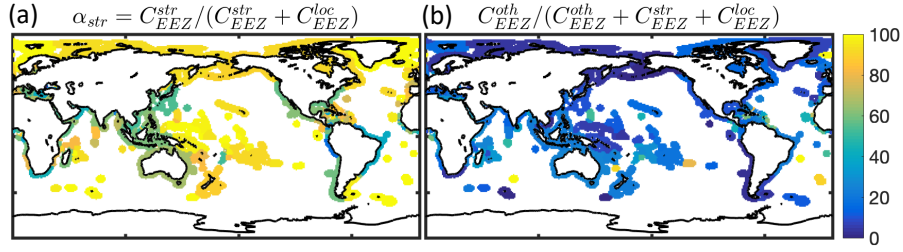


**Figure D1.** Straddling fraction of catches across EEZs during the 1990s (in %). (a) Fraction of catch on straddling species compared to catch on non straddling species  $\alpha_{str}$ . (b) Fraction of catch on species for which the identity is not provided (in %).

559 shows the estimated mean fraction of straddling catch per LME around the global peak  
 560 harvest of the 1990s. Note that for each region, a fraction of catch could not be linked  
 561 to species  $C_{EEZ}^{oth}$ , but this fraction is minimal in most EEZs (see Fig. D1b), and thus dis-  
 562 regarded in our analysis of the straddling catch fraction.

563 Figure D2 summarizes the effect of redistributing an increasing ratio  $\delta_s$  of catch  
 564 from the HS to the CS, in proportion to the fraction of simulated catch on straddling  
 565 species  $\alpha_{str}$  in each EEZ. It also shows the corresponding annual HS catches.

566 Increasing  $\delta_s$  has the expected effect of strongly reducing the HS vs. CS catch frac-  
 567 tion (Fig. D2a), up to matching observation for  $\delta_s = 0.5$ . Despite the improve-  
 568 ment, remain-  
 569 ing catches in the HS are significantly larger than what is observed ( $\sim 4 \cdot 10^6 MT/y$ ,  
 570 observation around peak of the 1990s, see Fig. D2b). We conclude that the biomass re-  
 571 distribution by migrating species alone does not explain the smaller exploitation of the  
 high seas, nevertheless it must have a significant impact.

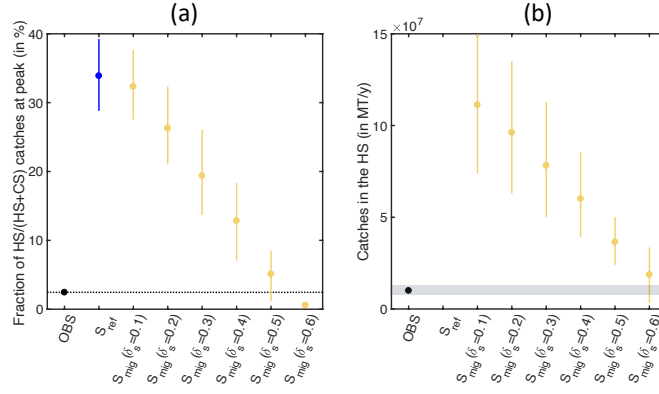


**Figure D2.** Effect of catch redistribution. (a) Observed and simulated fraction of HS vs. CS catches at global peak for multiple model variants. (b) Annual HS catch around the catch peak of the 1990s. Panels (a,b) show the ensemble mean as well as the 25-75th percentile ranges per simulation set compared to observation, black dot and horizontal dotted line.

572 **Appendix E Pelagic and Demersal catches in SAU**

573 We compare simulated pelagic and demersal catches with global catch reconstruction  
 574 from Sea Around Us (SAU) (Pauly et al., 2020). Table E1 lists how we distribute  
 575 the functional types of SAU to generate aggregated maps of pelagic and demersal catches.

**Table E1.** Association of SAU functional types to pelagic and demersal catches.

Catch type	SAU functional types
Pelagic	pelagic s/m/l
	bathypelagic s/m/l
	cephalopods
Demersal	demersal s/m/l
	reef-associated s/m/l
	benthopelagic s/m/l
	bathydemersal s/l
	shark s/l
	flatfish s/l
	ray s/l
	shrimp
	lobster and crab
other demersal invertebrates	

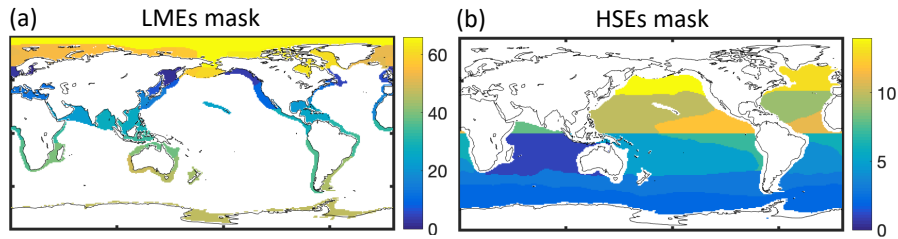


**Figure F1.** Regional masks to compare observation and simulation. (a) Large Marine Ecosystems. (b) High Seas Ecosystems adapted from Weber et al. (2016).

## Appendix F Large Marine Ecosystems and High Seas Ecosystems

Catch are compared across Large Marine Ecosystems (LMEs) for coastal regions, and 11 High Seas Ecosystems (HSEs). Figure F1a, b illustrate respectively the LME and HSE masks.

### Open Research Section

All data and the model used in this study are publicly available. Catch observation used for comparison of simulations can be obtained from the links <https://www.searoundus.org> and <http://dx.doi.org/10.4226/77/58293083b0515>. Biomass simulations from FishMIP can be obtained from the link <https://www.isimip.org/outputdata/>. Other processed data, as well as the code of the model BOATS used for this analysis, are available at the link <https://zenodo.org/records/10662929>.

### Acknowledgments

D.B. and J.G. acknowledge support from the US National Aeronautics and Space Administration (NASA) grant 80NSSC21K0420. Computational resources were provided by the Expanse system at the San Diego Supercomputer Center through allocation TG-OCE170017 from the Advanced Cyber infrastructure Coordination Ecosystem: Services and Support (ACCESS) program, which is supported by National Science Foundation grants 2138259, 2138286, 2138307, 2137603, and 2138296. E.D.G. was supported by the Canada Research Chairs Program fund number CRC-2020-00108. K.J.N.S was supported by the Norwegian Research Council, project 326896.

### References

- Amante, C., & Eakins, B. W. (2009). Etopo1 arc-minute global relief model: procedures, data sources and analysis.
- Bar-On, Y. M., Phillips, R., & Milo, R. (2018). The biomass distribution on earth. *Proceedings of the National Academy of Sciences*, 115(25), 6506–6511.
- Behrenfeld, M. J., & Falkowski, P. G. (1997). Photosynthetic rates derived from satellite-based chlorophyll concentration. *Limnology and Oceanography*, 42(1),

- 603 1–20.
- 604 Bianchi, D., Carozza, D. A., Galbraith, E. D., Quiet, J., & DeVries, T. (2021). Es-  
 605 timating global biomass and biogeochemical cycling of marine fish with and  
 606 without fishing. *Science advances*, *7*(41), eabd7554.
- 607 Blanchard, J. L., Heneghan, R. F., Everett, J. D., Trebilco, R., & Richardson, A. J.  
 608 (2017). From bacteria to whales: Using functional size spectra to model  
 609 marine ecosystems. *Trends in Ecology & Evolution*, *32*(3), 174–186. doi:  
 610 10.1016/j.tree.2016.12.003
- 611 Blanchard, J. L., Law, R., Castle, M. D., & Jennings, S. (2011). Coupled energy  
 612 pathways and the resilience of size-structured food webs. *Theoretical Ecology*,  
 613 *4*(3), 289–300. doi: 10.1007/s12080-010-0078-9
- 614 Block, B. A., Jonsen, I. D., Jorgensen, S. J., Winship, A. J., Shaffer, S. A., Bograd,  
 615 S. J., ... others (2011). Tracking apex marine predator movements in a  
 616 dynamic ocean. *Nature*, *475*(7354), 86.
- 617 Buesseler, K. O., & Boyd, P. W. (2009). Shedding light on processes that control  
 618 particle export and flux attenuation in the twilight zone of the open ocean.  
 619 *Limnology and Oceanography*, *54*(4), 1210–1232.
- 620 Carozza, D. A., Bianchi, D., & Galbraith, E. D. (2016). The ecological module  
 621 of BOATS-1.0: a bioenergetically constrained model of marine upper trophic  
 622 levels suitable for studies of fisheries and ocean biogeochemistry. *Geoscientific*  
 623 *Model Development*, *9*(4), 1545–1565.
- 624 Carozza, D. A., Bianchi, D., & Galbraith, E. D. (2017, 01). Formulation, general  
 625 features and global calibration of a bioenergetically-constrained fishery model.  
 626 *PLOS One*, *12*(1), 1–28. doi: 10.1371/journal.pone.0169763
- 627 Carr, M.-E., Friedrichs, M. A., Schmeltz, M., Aita, M. N., Antoine, D., Arrigo,  
 628 K. R., ... others (2006). A comparison of global estimates of marine primary  
 629 production from ocean color. *Deep Sea Research Part II: Topical Studies in*  
 630 *Oceanography*, *53*(5), 741–770.
- 631 Cullis-Suzuki, S., & Pauly, D. (2010). Failing the high seas: A global evaluation  
 632 of regional fisheries management organizations. *Marine Policy*, *34*(5), 1036 -  
 633 1042. doi: <https://doi.org/10.1016/j.marpol.2010.03.002>
- 634 Dunne, J. P., Armstrong, R. A., Gnanadesikan, A., & Sarmiento, J. L. (2005).  
 635 Empirical and mechanistic models for the particle export ratio. *Global Biogeo-*  
 636 *chemical Cycles*, *19*(4).
- 637 Eddy, T. D., Bernhardt, J. R., Blanchard, J. L., Cheung, W. W., Colléter, M.,  
 638 Du Pontavice, H., ... others (2020). Energy flow through marine ecosystems:  
 639 Confronting transfer efficiency. *Trends in Ecology & Evolution*.
- 640 Eigaard, O. R., Marchal, P., Gislason, H., & Rijnsdorp, A. D. (2014). Technological  
 641 development and fisheries management. *Reviews in Fisheries Science & Aqua-*  
 642 *culture*, *22*(2), 156–174.
- 643 Galbraith, E. D., Carozza, D. A., & Bianchi, D. (2017). A coupled human-earth  
 644 model perspective on long-term trends in the global marine fishery. *Nature*  
 645 *Communications*, *8*, 14884.
- 646 Galbraith, E. D., Le Mézo, P., Solanes Hernandez, G., Bianchi, D., & Kroodsma, D.

- 647 (2019). Growth limitation of marine fish by low iron availability in the open  
648 ocean. *Frontiers in Marine Science*, 509.
- 649 Gjerde, K., Reeve, L., Harden-Davies, H., Ardron, J., Dolan, R., Durussel, C., ...  
650 others (2016). Protecting earth's last conservation frontier: scientific, manage-  
651 ment and legal priorities for mpas beyond national boundaries.
- 652 Golden, C. D., Koehn, J. Z., Shepon, A., Passarelli, S., Free, C. M., Viana, D. F., ...  
653 others (2021). Aquatic foods to nourish nations. *Nature*, 598(7880), 315–320.
- 654 Guiet, J., Aumont, O., Poggiale, J.-C., & Maury, O. (2016). Effects of lower trophic  
655 level biomass and water temperature on fish communities: A modelling study.  
656 *Progress in Oceanography*, 146, 22 - 37. doi: [http://dx.doi.org/10.1016/](http://dx.doi.org/10.1016/j.pocean.2016.04.003)  
657 [j.pocean.2016.04.003](http://dx.doi.org/10.1016/j.pocean.2016.04.003)
- 658 Guiet, J., Bianchi, D., Scherrer, K. J., Heneghan, R. F., & Galbraith, E. D. (2024).  
659 Boatsv2: New ecological and economic features improve simulations of high  
660 seas catch and effort. *Submitted in Geoscientific Model Development*.
- 661 Guiet, J., Galbraith, E. D., Bianchi, D., & Cheung, W. W. (2020). Bioenergetic in-  
662 fluence on the historical development and decline of industrial fisheries. *ICES*  
663 *Journal of Marine Science*, 77(5), 1854–1863.
- 664 Haedrich, R. L., & Merrett, N. R. (1992). Production/biomass ratios, size frequen-  
665 cies and biomass spectra in deep-sea demersal fishes. In *Deep-sea food chains*  
666 *and the global carbon cycle* (pp. 157–182). Springer.
- 667 Hatton, I. A., Heneghan, R. F., Bar-On, Y. M., & Galbraith, E. D. (2021). The  
668 global ocean size spectrum from bacteria to whales. *Science Advances*, 7(46),  
669 eabh3732. doi: 10.1126/sciadv.abh3732
- 670 Heilpern, S. A., DeFries, R., Fiorella, K., Flecker, A., Sethi, S. A., Uriarte, M., &  
671 Naeem, S. (2021). Declining diversity of wild-caught species puts dietary  
672 nutrient supplies at risk. *Science Advances*, 7(22), eabf9967.
- 673 Helm, R. R. (2022). Turning the tide on high-seas plastic pollution. *One Earth*,  
674 5(10), 1089–1092.
- 675 Heneghan, R. F., Galbraith, E., Blanchard, J. L., Harrison, C., Barrier, N., Bulman,  
676 C., ... others (2021). Disentangling diverse responses to climate change among  
677 global marine ecosystem models. *Progress in Oceanography*, 198, 102659.
- 678 Irigoien, X., Klevjer, T. A., Røstad, A., Martinez, U., Boyra, G., & et al., A. J. L.  
679 (2014). Large mesopelagic fishes biomass and trophic efficiency in the open  
680 ocean. *Nature Communications*, 5.
- 681 Juan-Jordá, M. J., Murua, H., Arrizabalaga, H., Merino, G., Pacoureau, N., &  
682 Dulvy, N. K. (2022). Seventy years of tunas, billfishes, and sharks as sentinels  
683 of global ocean health. *Science*, 378(6620), eabj0211.
- 684 Kerry, C. R., Exeter, O. M., & Witt, M. J. (2022). Monitoring global fishing activ-  
685 ity in proximity to seamounts using automatic identification systems. *Fish and*  
686 *Fisheries*, 23(3), 733–749.
- 687 Kvile, K. Ø., Taranto, G. H., Pitcher, T. J., & Morato, T. (2014). A global as-  
688 sessment of seamount ecosystems knowledge using an ecosystem evaluation  
689 framework. *Biological Conservation*, 173, 108–120.
- 690 Lam, V. W. Y., Sumaila, U. R., Dyck, A., Pauly, D., & Watson, R. (2011). Con-

- 691       struction and first applications of a global cost of fishing database. *ICES Jour-*  
692       *nal of Marine Science*, 68(9), 1996-2004. doi: 10.1093/icesjms/fsr121
- 693 Le Mézo, P. K., & Galbraith, E. D. (2021). The fecal iron pump: global impact of  
694 animals on the iron stoichiometry of marine sinking particles. *Limnology and*  
695       *Oceanography*, 66(1), 201–213.
- 696 Locarnini, R. A., Mishonov, A. V., Antonov, J. I., Boyer, T. P., & Garcia, H. E.  
697 (2006). World ocean atlas 2005, volume 1: Temperature. s. levitus. *Ed. NOAA*  
698       *Atlas NESDIS 61, U.S. Government Printing Office, Washington, D.C., 182*  
699       *pp.*
- 700 Lotze, H. K., Tittensor, D. P., Bryndum-Buchholz, A., Eddy, T. D., Cheung,  
701       W. W. L., Galbraith, E. D., . . . Worm, B. (2019). Global ensemble pro-  
702       jections reveal trophic amplification of ocean biomass declines with cli-  
703       mate change. *Proceedings of the National Academy of Sciences*. doi:  
704       10.1073/pnas.1900194116
- 705 Marra, J., Trees, C. C., & O'Reilly, J. E. (2007). Phytoplankton pigment absorption:  
706       a strong predictor of primary productivity in the surface ocean. *Deep Sea Re-*  
707       *search Part I: Oceanographic Research Papers*, 54(2), 155–163.
- 708 Martin, J. H., Knauer, G. A., Karl, D. M., & Broenkow, W. W. (1987). Vertex: car-  
709       bon cycling in the northeast pacific. *Deep Sea Research Part A. Oceanographic*  
710       *Research Papers*, 34(2), 267–285.
- 711 Maury, O. (2010). An overview of apecosm, a spatialized mass balanced “apex  
712       predators ecosystem model” to study physiologically structured tuna pop-  
713       ulation dynamics in their ecosystem. *Progress in Oceanography*, 84(1-2),  
714       113–117.
- 715 Moore, C., Mills, M., Arrigo, K., Berman-Frank, I., Bopp, L., Boyd, P., . . . oth-  
716       ers (2013). Processes and patterns of oceanic nutrient limitation. *Nature*  
717       *geoscience*, 6(9), 701–710.
- 718 Nuno, A., Guiet, J., Baranek, B., & Bianchi, D. (2022). Patterns and drivers of the  
719       diving behavior of large pelagic predators. *bioRxiv*. doi: [https://doi.org/10](https://doi.org/10.1101/2022.12.27.521953)  
720       .1101/2022.12.27.521953
- 721 Pacoureau, N., Rigby, C. L., Kyne, P. M., Sherley, R. B., Winker, H., Carlson, J. K.,  
722       . . . others (2021). Half a century of global decline in oceanic sharks and rays.  
723       *Nature*, 589(7843), 567–571.
- 724 Palomares, M. L., & Pauly, D. (2019). On the creeping increase of vessels’ fishing  
725       power. *Ecology and Society*, 24(3).
- 726 Pauly, D., Zeller, D., & Palomares, M. (2020). Sea around us concepts, design and  
727       data. Retrieved from [searoundus.org](http://searoundus.org)
- 728 Petrik, C. M., Stock, C. A., Andersen, K. H., van Denderen, P. D., & Watson, J. R.  
729       (2019). Bottom-up drivers of global patterns of demersal, forage, and pelagic  
730       fishes. *Progress in oceanography*, 176, 102124.
- 731 Proud, R., Cox, M. J., Le Guen, C., & Brierley, A. S. (2018). Fine-scale depth struc-  
732       ture of pelagic communities throughout the global ocean based on acoustic  
733       sound scattering layers. *Marine Ecology Progress Series*, 598, 35–48.
- 734 RAM Legacy Stock Assessment Database. (2020). *Ram legacy stock assessment*

- 735        *database v4.491*. Retrieved from <https://doi.org/10.5281/zenodo.3676088>  
736        doi: 10.5281/zenodo.3676088
- 737        Rousseau, Y., Watson, R. A., Blanchard, J. L., & Fulton, E. A. (2019). Evolution  
738        of global marine fishing fleets and the response of fished resources. *Proceedings*  
739        *of the National Academy of Sciences*, *116*(25), 12238–12243. doi: 10.1073/pnas  
740        .1820344116
- 741        Sala, E., Mayorga, J., Bradley, D., Cabral, R. B., Atwood, T. B., Auber, A., ...  
742        others (2021). Protecting the global ocean for biodiversity, food and climate.  
743        *Nature*, *592*(7854), 397–402.
- 744        Sala, E., Mayorga, J., Costello, C., Kroodsma, D., Palomares, M. L., Pauly, D., ...  
745        Zeller, D. (2018). The economics of fishing the high seas. *Science advances*,  
746        *4*(6), eaat2504.
- 747        Scherrer, K., & Galbraith, E. D. (2020). Regulation strength and technology creep  
748        play key roles in global long-term projections of wild capture fisheries. *ICES*  
749        *Journal of Marine Science*. doi: 10.1093/icesjms/fsaa109
- 750        Scherrer, K. J., Rousseau, Y., Teh, L. C., Sumaila, U. R., & Galbraith, E. D. (2023).  
751        Diminishing returns on labour in the global marine food system. *Nature Sus-*  
752        *tainability*, 1–8.
- 753        Schiller, L., Bailey, M., Jacquet, J., & Sala, E. (2018). High seas fisheries play a  
754        negligible role in addressing global food security. *Science Advances*, *4*(8),  
755        eaat8351.
- 756        Stasko, A. D., Swanson, H., Majewski, A., Atchison, S., Reist, J., & Power, M.  
757        (2016). Influences of depth and pelagic subsidies on the size-based trophic  
758        structure of beaufort sea fish communities. *Marine Ecology Progress Series*,  
759        *549*, 153–166.
- 760        Stock, C. A., John, J. G., Rykaczewski, R. R., Asch, R. G., Cheung, W. W. L.,  
761        Dunne, J. P., ... Watson, R. A. (2017). Reconciling fisheries catch and ocean  
762        productivity. *Proceedings of the National Academy of Sciences*, *114*(8), E1441-  
763        E1449. doi: 10.1073/pnas.1610238114
- 764        Sumaila, U. R., Lam, V. W., Miller, D. D., Teh, L., Watson, R. A., Zeller, D., ...  
765        others (2015). Winners and losers in a world where the high seas is closed to  
766        fishing. *Scientific Reports*, *5*(1), 1–6.
- 767        Sutton, T., Porteiro, F., Heino, M., Byrkjedal, I., Langhelle, G., Anderson, C., ...  
768        others (2008). Vertical structure, biomass and topographic association of deep-  
769        pelagic fishes in relation to a mid-ocean ridge system. *Deep Sea Research Part*  
770        *II: Topical Studies in Oceanography*, *55*(1-2), 161–184.
- 771        Tagliabue, A., Bowie, A. R., Boyd, P. W., Buck, K. N., Johnson, K. S., & Saito,  
772        M. A. (2017). The integral role of iron in ocean biogeochemistry. *Nature*,  
773        *543*(7643), 51–59.
- 774        Tittensor, D. P., Eddy, T. D., Lotze, H. K., Galbraith, E. D., Cheung, W., Barange,  
775        M., ... others (2018). A protocol for the intercomparison of marine fishery and  
776        ecosystem models: Fish-mip v1. 0. *Geoscientific Model Development*, *11*(4),  
777        1421–1442.
- 778        Tittensor, D. P., Novaglio, C., Harrison, C. S., Heneghan, R. F., Barrier, N.,

- 779            Bianchi, D., ... others (2021). Next-generation ensemble projections reveal  
780            higher climate risks for marine ecosystems. *Nature Climate Change*, 11(11),  
781            973–981.
- 782            Trueman, C., Johnston, G., O’hea, B., & MacKenzie, K. (2014). Trophic interactions  
783            of fish communities at midwater depths enhance long-term carbon storage and  
784            benthic production on continental slopes. *Proceedings of the Royal Society B:  
785            Biological Sciences*, 281(1787), 20140669.
- 786            van Denderen, P. D., Lindegren, M., MacKenzie, B. R., Watson, R. A., & Andersen,  
787            K. H. (2018). Global patterns in marine predatory fish. *Nature ecology &  
788            evolution*, 2(1), 65.
- 789            Watson, R. A. (2017). A database of global marine commercial, small-scale, illegal  
790            and unreported fisheries catch 1950–2014. *Scientific Data*, 4.
- 791            Watson, R. A., & Morato, T. (2013). Fishing down the deep: Accounting for within-  
792            species changes in depth of fishing. *Fisheries Research*, 140, 63–65.
- 793            Weber, T., Cram, J. A., Leung, S. W., DeVries, T., & Deutsch, C. (2016). Deep  
794            ocean nutrients imply large latitudinal variation in particle transfer efficiency.  
795            *Proceedings of the National Academy of Sciences*, 113(31), 8606–8611.
- 796            White, C., & Costello, C. (2014). Close the high seas to fishing? *PLoS biology*,  
797            12(3), e1001826.
- 798            Worm, B., & Branch, T. A. (2012). The future of fish. *Trends in Ecology & Evolu-  
799            tion*, 27(11), 594 - 599. doi: <https://doi.org/10.1016/j.tree.2012.07.005>